DISCLAIMER

This report was prepared as an account of work sponsored by an agency of the United States Government. Neither the United States Government nor any agency thereof, nor any of their employees, makes any warranty, express or implied, or assumes any legal liability or responsibility for the accuracy, completeness, or usefulness of any information, apparatus, product, or process disclosed, or represents that its use would not infringe privately owned rights. Reference herein to any specific commercial product, process, or service by trade name, trademark, manufacturer, or otherwise does not necessarily constitute or imply its endorsement, recommendation, or favoring by the United States Government or any agency thereof. The views and opinions of authors expressed herein do not necessarily state or reflect those of the United States Government or any agency thereof. Reference herein to any social initiative (including but not limited to Diversity, Equity, and Inclusion (DEI); Community Benefits Plans (CBP); Justice 40; etc.) is made by the Author independent of any current requirement by the United States Government and does not constitute or imply endorsement, recommendation, or support by the United States Government or any agency thereof.

SANDIA REPORT
SAND2025-14944
Printed December 2025

Sandia National Laboratories

Cable/Antenna Bounds Connecting Field Levels To Personnel Safety And Electronic Upset Thresholds

Larry K. Warne, William L. Langston, and Luis San Martin

Prepared by
Sandia National Laboratories
Albuquerque, New Mexico
87185 and Livermore,
California 94550

Issued by Sandia National Laboratories, operated for the United States Department of Energy by National Technology & Engineering Solutions of Sandia, LLC.

Available to DOE and DOE contractors from
U.S. Department of Energy
Office of Scientific and Technical Information
P.O. Box 62
Oak Ridge, TN 37831

Telephone: (865) 576-8401
Facsimile: (865) 576-5728
E-Mail: reports@osti.gov
Online ordering: http://www.osti.gov/scitech

Available to the public from
U.S. Department of Commerce
National Technical Information Service
5301 Shawnee Rd
Alexandria, VA 22312

Telephone: (800) 553-6847
Facsimile: (703) 605-6900
E-Mail: orders@ntis.gov
Online order: https://classic.ntis.gov/help/order-methods/

SAND2025-14944

Unlimited Release

Printed December 2025

Cable/Antenna Bounds Connecting Field Levels To Personnel Safety And Electronic Upset Thresholds

L. K. Warne and W. L. Langston, Plasma/EM Software Dept.
Luis San martin, EM/Electronics Analyses Dept.
Sandia National Laboratories
P. O. Box 5800
Albuquerque, NM 87185-1152

December 4, 2025

Abstract

We use bounding models to estimate the power delivered to interior ordnance as well as the pin level voltages along a cable at interior electronic components. The procedures underlying these estimates are described in some detail. Conservation of steady-state power in a linear passive system underpins the power estimate, whereas, losses and quality factor limits underpin the limits on voltage transformations. The final levels are compared to no-fire threshold power and to minimum upset voltage levels in an example using a canonical slot aperture and cavity to estimate interior fields.

This page left blank

Contents

List of Figures

This page left blank

1 INTRODUCTION

This report discusses bounding estimates of cable coupling and resulting pin-level power and voltage. The next section considers the electronic upset problem and gives formulas for estimating maximum pin-level voltages on a cable subjected to an incident field level. This section begins with an unshielded cable and touches on the effect of a cable shield (the second appendix has more discussion on a shielded cable) along with a brief discussion of cable effective height measurements. The section that follows discusses the personnel safety problem and estimates for worst case power to ordnance using the V-curve matched load argument. Using results from the first appendix the next section considers a simple example of electromagnetic penetration of a canonical exterior shield through a slot to establish the interior field levels in a canonical overmoded cavity, focusing on the higher frequency region of the Electromagnetic Radiation (EMR) Environment, to estimate induced cable voltage levels and coupled device power (in addition to transmitted power through the shield). The next section briefly discusses screening levels of the electronics upset voltage threshold and typical ordnance power thresholds. The final conclusion section summarizes the results. The formulas provided in this report can be readily applied to actual geometries following the procedures given for the example here.

This page left blank

2 CABLE COUPLING AND UPSET

To assess the possibility of voltage upset of electronics, we will examine the coupling to a model of the cable leading to the vulnerable device. Realistic losses will be inserted on the cable, which limit the wiring quality factor, and subsequently limit voltage transformations along the cable up to the vulnerable device. We will also consider drives of cables from collections of plane waves and show that the result is slightly reduced from the preceding maximum case.

The cable coupling will actually be addressed in two ways. First, we will estimate the differential/common mode coupling to an unshielded cable as a limiting case of poor shielding. The second appendix will discuss a shielded cable. We will also briefly discuss effective height and impedance measurements of typical cables below.

2.1 Unshielded Cable

Let us first consider coupling to the differential mode of a balanced twin conductor cable. We use the transverse drive equations (this approach includes the effect of the transverse field at the ends of the cable) [1], [2]. The voltage equation is (harmonic time dependence $e^{-i\omega t}$ is suppressed throughout)

$$\frac{dV}{dz} = -ZI - i\omega L^i H_\perp^{ext} \tag{1}$$

with impedance per unit length

$$Z = R - iX = 2Z^{fi} - i\omega L_e \tag{2}$$

For two equal radius cylindrical conductors of radius a and separation D [3] the inductance per unit length is

$$L_e = \frac{\mu_0}{\pi}\text{Arccosh}\left(\frac{D}{2a}\right) \sim \frac{\mu_0}{\pi}\ln\left(D/a\right)\ ,\ D >> 2a \tag{3}$$

and the finitely conducting internal impedance per unit length due to skin-effect ($\delta << a$) is

$$Z^{fi} = \frac{Z_s}{2\pi a}\left[\frac{D/\left(2a\right)}{\sqrt{D^2/\left(2a\right)^2 - 1}}\right] \sim \frac{Z_s}{2\pi a}\ ,\ D >> 2a \tag{4}$$

where

$$Z_s = \left(1 - i\right)R_s \tag{5}$$

$$R_s = 1/\left(\delta\sigma\right) \tag{6}$$

$$\delta = \sqrt{2/\left(\omega\mu\sigma\right)} \tag{7}$$

with [1]

$$L^i/\mu_0 = 2h_e \tag{8}$$

Note that for the limit $\delta >> a$ the resistance per unit length per conductor $\text{Re}\left(Z^{fi}\right)$is $R^{fi} \sim 1/\left(\pi a^2\sigma\right)$.

The current equation is

$$\frac{dI}{dz} = -YV + i\omega C^i E_\perp^{ext} \tag{9}$$

with admittance per unit length

$$Y = G - i\omega C \tag{10}$$

The propagation constant is

$$\Gamma = \sqrt{-ZY} = \Gamma' + i\Gamma'' \tag{11}$$

and the characteristic impedance is

$$Z_0 = \sqrt{Z/Y} \approx \sqrt{L/C} \tag{12}$$

where

$$\sqrt{L/C} = \frac{\eta}{\pi}\text{Arccosh}\left(\frac{D}{2a}\right) \sim \frac{\eta}{\pi}\ln\left(D/a\right)\ ,\ D >> 2a \tag{13}$$

with the intrinsic impedance

$$\eta = \sqrt{\mu_0/\varepsilon} \tag{14}$$

The capacitance per unit length [3] is

$$C = \pi\varepsilon/\text{Arccosh}\left(\frac{D}{2a}\right) \sim \pi\varepsilon/\ln\left(D/a\right)\ ,\ D >> 2a \tag{15}$$

where we can estimate the conductance per unit length from the dielectric loss tangent (assuming the dielectric fills the space between conductors)

$$G/\left(\omega C\right) = \tan\delta \tag{16}$$

and for a homogeneous dielectric [1]

$$C^i/\varepsilon = 2h_e C/\varepsilon = 2h_e\eta/\sqrt{L/C} \tag{17}$$

with charge and current centroid position h_e

$$2h_e/D = \sqrt{1-\left(2a/D\right)^2} \sim 1\ ,\ D >> 2a \tag{18}$$

Let us first take the incident electric field to be parallel to the plane containing the wire axes [1]

$$H_\perp^{ext} = H_0 e^{ik_0 z\cos\theta_0} \tag{19}$$

$$E_\perp^{ext} = E_0\cos\theta_0 e^{ik_0 z\cos\theta_0} \tag{20}$$

where the wavenumber of the transmission line is

$$k = \omega\sqrt{\mu_0\varepsilon} = \omega\sqrt{LC} \tag{21}$$

and the free space wavenumber is

$$k_0 = \omega\sqrt{\mu_0\varepsilon_0} \tag{22}$$

with

$$E_0 = \eta_0 H_0 \tag{23}$$

The transmission line equations then become

$$\frac{dV}{dz} + ZI = -i\omega L^i H_\perp^{ext} = -ik2h_e \eta H_0 e^{ik_0 z\cos\theta_0} \tag{24}$$

$$\frac{dI}{dz} + YV = i\omega C^i E_\perp^{ext} = ik2h_e \frac{E_0\cos\theta_0}{\sqrt{L/C}} e^{ik_0 z\cos\theta_0} \tag{25}$$

and we are approximating for small losses along the line $\omega L >> R$, $\omega C >> G$. Eliminating the current gives

$$\frac{d^2V}{dz^2} - ZYV = \left(\frac{d^2V}{dz^2} + \Gamma^2\right) V = -i\omega C^i Z E_\perp^{ext} - i\omega L^i \frac{d}{dz} H_\perp^{ext}$$

$$= \omega\left(L^i k_0 H_0 - iC^i Z E_0\right)\cos\theta_0 e^{ik_0 z\cos\theta_0} \tag{26}$$

or for small losses $Z = R - i\omega L \approx -i\omega L$ approximately

$$\left(\frac{d^2V}{dz^2} + \Gamma^2\right) V \approx \left(\omega L^i k_0 H_0 - \frac{C^i}{C}\omega^2 LCE_0\right)\cos\theta_0 e^{ik_0 z\cos\theta_0}$$

$$\approx \left(\frac{L^i}{\mu_0} k_0^2 \eta_0 H_0/E_0 - \frac{C^i}{C}k^2\right) E_0\cos\theta_0 e^{ik_0 z\cos\theta_0}$$

$$\approx \left(2h_e k_0^2 \eta_0 H_0/E_0 - \frac{C^i}{C}k^2\right) E_0\cos\theta_0 e^{ik_0 z\cos\theta_0} \tag{27}$$

The solution is then

$$V(z) = c_0\cos(\Gamma z) + c_1\sin(\Gamma z)$$

$$+\left(\frac{\varepsilon_0}{\varepsilon}\eta_0 H_0/E_0 - 1\right)\left(2h_e\frac{k_0^2}{k^2}\eta_0 H_0/E_0 - \frac{C^i}{C}\right) E_0\cos\theta_0 e^{ik_0 z\cos\theta_0} k^2/\left(\Gamma^2 - k_0^2\cos^2\theta_0\right) \tag{28}$$

In the homogeneous case $k_0 \to k$ and $C^i/C \to 2h_e$, in which case $2h_e\left(k_0^2\eta_0 H_0/E_0 - k^2\right)$ vanishes, and then the solution is

$$V(z) = c_0\cos(\Gamma z) + c_1\sin(\Gamma z) \tag{29}$$

Below we investigate general incidence and polarization angles, as well as a random collection of plane waves as would be found in a high frequency cavity. The results are very similar to this simple case where the wave vector and electric field vector are in the plane containing the twin wire line. If we take as boundary conditions a short circuit on the left end and an open circuit on the right end (note that we are at high frequencies here with half-wave oscillations along the cable, so that this precise choice is not critical)

$$V(0) = I(\ell) = 0 \tag{30}$$

then $c_0 = 0$ as well as

$$\frac{dV}{dz}(\ell) + ZI(\ell) = c_1\Gamma\cos(\Gamma\ell) = -ik2h_e\eta_0 H_0 e^{ik\ell\cos\theta_0} \tag{31}$$

and therefore

$$V(z) = -i(k/\Gamma)\, 2h_e\eta_0 H_0 e^{ik\ell\cos\theta_0}\frac{\sin(\Gamma z)}{\cos(\Gamma\ell)} \tag{32}$$

and if we take $\Gamma \to k$ in the amplitude factor

$$V(\ell) \approx -i2h_e\eta_0 H_0 e^{ik\ell\cos\theta_0}\tan(\Gamma\ell) \tag{33}$$

If we examine the resonant limit $\Gamma'\ell \to (n-1/2)\,\pi$ where the dominant real part is ($\Gamma'' << \Gamma'$)

$$\Gamma' \approx \omega\sqrt{LC} = k \tag{34}$$

the small imaginary part can be written in terms of the losses as

$$\Gamma'' \approx \frac{\Gamma'}{2}\left(\frac{R}{\omega L}+\frac{G}{\omega C}\right) = \frac{\Gamma'}{2}\left(1/Q_R + \tan\delta\right) = \Gamma'/(2Q) \tag{35}$$

where the quality factor Q is a combination of losses from the conductors Q_R, the dielectric Q_D, radiation Q_{rad}, etc.

$$1/Q = 1/Q_R + 1/Q_D + 1/Q_{rad} + \cdots = 1/Q_R + \tan\delta + 1/Q_{rad} + \cdots \tag{36}$$

Then we find

$$\cos(\Gamma\ell) \approx \cos(\Gamma'\ell) - i\Gamma''\ell\sin(\Gamma'\ell) \approx -i\Gamma''\ell\,(-1)^{n-1} = -i\,(-1)^{n-1}\,\Gamma'\ell/(2Q) \tag{37}$$

Taking the real part to approach $\Gamma' \to k$

$$V(\ell)\,k\ell/(2Q) \approx 2h_e\eta_0 H_0 e^{ik\ell\cos\theta_0} \tag{38}$$

or (unity if sufficiently lossy)

$$\left|\frac{V(\ell)}{2h_e\eta_0 H_0}\right| \approx \frac{1}{\Gamma''\ell} \approx \frac{2Q}{k\ell} \tag{39}$$

The maximum as a function of incident angles is then the normal incidence result

$$\left|V(\ell)\,k\ell/(2Q)\right|_{\max} \approx 2h_e\eta_0 H_0 \tag{40}$$

2.2 Cable Common Mode Generalizations And Resonances

The maximum voltage is thus magnified by the resonant quality factor Q, but the electrical length $k\ell$ can also be large (tending to reduce the voltage). What we are really saying here is that the losses lead to a bounding quality factor, which limits the voltage transformations. The wire spacing D is relatively small so the balanced differential mode voltage is relatively small.

If there is efficient common-to-differential mode conversion then the common mode coupling is also of interest. If we are talking about a wire with respect to a cable braid shield, then the spacing D is replaced by the wire spacing from the cable braid to the image in the cable braid, but the impedance per unit length, the distributed voltage source, and the voltage, are cut in half. If we are instead talking about the coupling to the cable braid with respect to the chassis wall, then the radius a is replaced by the equivalent radius of the cable a_c, and the spacing D is replaced by the distance to the image in the chassis wall D_c, but the impedance per unit length, the distributed voltage source, and the voltage, are again cut in half. If such common-to-differential mode conversion were present (so that common mode signals were delivered to

differential circuits), the most important feature of the coupling in (38) is the effective separation h_e (related to D), which could be increased in the common mode coupling geometry. In both these cases, the tangential magnetic field drive near the wall H_0 can in principle be increased due to the conductive boundary condition there, however, if a braided shield is present these modes require penetration of the braid to provide such a drive, and consequently bring in the cable shielding and resulting reduction of H_0 into the calculation (these coupling levels may be down by an order of magnitude or more). The second appendix briefly discusses the braided cable coupling.

We have assumed here that the cable is single-moded even when we are operating at high frequencies; for a one-dimensional resonator, the relative modal spacing $\Delta k/k = \pi/(k\ell) = 1/(n-1/2)$ can be larger than the 3 dB width $\Delta k_3/k = 1/Q$, if the quality factor Q is very large. The voltage magnification factor here (38)

$$\pi Q/(k\ell) = \Delta k/\Delta k_3 \tag{41}$$

is the ratio of the modal spacing to the 3 dB width; this value shrinks with increasing frequency even in the case of this one-dimensional resonant system. If coupling to additional TEM modes in the multiconductor cable are taken into account, introducing additional resonant modes, we expect it to shrink further.

2.3 Damping Mechanisms And Q

The cable system quality factor Q is now estimated, where it is defined as the radian frequency times the peak energy stored W, divided by the average power lost P [3]

$$Q = \frac{\omega W}{P} \tag{42}$$

The prior values of the quality factor for dielectric losses is determined from the loss tangent of the material

$$Q_D = 1/\tan\delta \tag{43}$$

Some values are known for fairly high frequencies such as 25 GHz [4]. For example, Teflon has $\tan\delta \approx 6\times 10^{-4}$ and $Q_D \approx 1667$; at 10 GHz $\tan\delta \approx 3.7\times 10^{-4}$ and $Q_D \approx 2703$; at 3 GHz $\tan\delta \approx 1.5\times 10^{-4}$ and $Q_D \approx 6667$.

The conductor ohmic losses for the example of 20 AWG copper wire with [5] $2a = 0.032$ inches (the stranded case has $2a \approx 0.040$ inches), $\sigma = 5.8\times 10^7$ S/m give

$$Q_R \approx \frac{\omega L}{R} \approx \frac{\omega\mu_0 a}{R_s}\text{Arccosh}\left(\frac{D}{2a}\right)\left[\frac{\sqrt{D^2/(2a)^2-1}}{D/(2a)}\right] \sim \frac{\omega\mu_0 a\ln(D/a)}{R_s} = \frac{2a\ln(D/a)}{\delta}\ ,\ D >> 2a\ ,\ \mu = \mu_0 \tag{44}$$

For a wire-to-wire spacing $D = 0.06$ inches we find at 25 GHz that $Q_R \approx 2042$; at 10 GHz $Q_R \approx 1292$; at 3 GHz $Q_R \approx 707.5$. Combining these two loss effects we find the quality factor due to absorption at 25 GHz

$$1/Q_{abs} = 1/Q_R + 1/Q_D \approx 917.7 \tag{45}$$

at 10 GHz $Q_{abs} \approx 874.2$; at 3 GHz $Q_{abs} \approx 639.6$. Generalizations of the ohmic losses to rectangular conductor geometries are summarized in the subsection below.

For the radiation damping, which has the form of lumped loads at the ends of the line, we estimate the stored electric energy along the cable (where the factor of one half accounts for the sinusoidal variation along the cable length and the subsection below briefly discusses alternate end conditions)

$$W_e = \int_0^\ell C\,|V(z)|^2\,dz = \frac{1}{2}\ell C\,|V(\ell)|^2 \tag{46}$$

and use [6]

$$P = \frac{1}{2} G_{rad} \left| V(\ell) \right|^2 + \frac{1}{2} R_{rad} \left| I(0) \right|^2 = G_{rad} \left| V(\ell) \right|^2 \tag{47}$$

For an extended exterior

$$G_{rad} Z_0^2 = \eta_0 \left(k h_e \right)^2 / (2\pi) = R_{rad} \tag{48}$$

to obtain

$$Q_{rad} \approx \frac{\ell \omega C}{2 G_{rad}} = \frac{\ell \omega L}{2 Z_0^2 G_{rad}} = \frac{k\ell \text{Arccosh}\left(\frac{D}{2a}\right)}{\left(k h_e\right)^2} \sim \frac{4 k\ell \ln(D/a)}{(kD)^2} \ , \ D >> 2a \tag{49}$$

Note that, this radiation damping inside a closed three-dimensional cavity volume still holds if the cavity is overmoded at very high frequencies. The lengths of the cables (or branches) are taken to be greater than one foot (and we note that there will exist some coupling at higher frequencies to remaining cable branches if they exist). For the same frequency and dimensions, with $\ell = 12$ inches, at 25 GHz, this gives $Q_{rad} \approx 1738$. The total is then

$$1/Q = 1/Q_{abs} + 1/Q_{rad} \tag{50}$$

Table 1 shows values for this example

f (GHz)	Q_R	Q_D	Q_{abs}	Q_{rad}	Q	$\pi Q/(k\ell)$	$\lvert V(\ell)/E_0 \rvert$ (m)
0.1	129.2	5000	125.9	4.289×10^6	125.9	619	0.51
0.3	223.7	6667	216.5	1.449×10^5	216.1	354	0.29
3.0	707.5	6667	639.6	1.449×10^4	612.6	100	0.082
10.0	1292	2703	874.0	4346	727.7	35.8	0.029
25.0	2042	1667	917.8	1738	600.6	11.8	0.0097

Table 1. Example quality factors and voltages for two wire line.

Note that this radiation damping is usually eliminated for the differential mode in a shielded cable. However, for a multi-pin cable (with N TEM modes) at high frequencies, perturbations of the invariant axial geometry lead to coupling between the various TEM modes, which introduce a level of damping having similar characteristics to the radiation damping.

Nevertheless, we plan to stick with only the absorption damping here. If we extrapolate from lower frequencies to 25 GHz and above we might take a bounding total quality factor

$$Q \approx Q_{abs} \leq 1000 \tag{51}$$

If we take a typical minimum cable length of $\ell = 12$ inches, a wire-to-wire spacing $D \approx 0.06$ inches with $2a \approx 0.032$ inches, 25 GHz frequency,and a quality factor $Q \approx 1000$ due to a combination of absorptive losses, we see that a differential mode will have a port voltage

$$\left| V(\ell) \right| \approx \frac{2Q}{k\ell} 2 h_e E_0 \approx 0.016 \text{ m } E_0 \ , \ 25 \text{ GHz} \tag{52}$$

with modal spacing-to-modal width

$$\Delta k / \Delta k_3 = \pi Q / (k\ell) \approx 20 \tag{53}$$

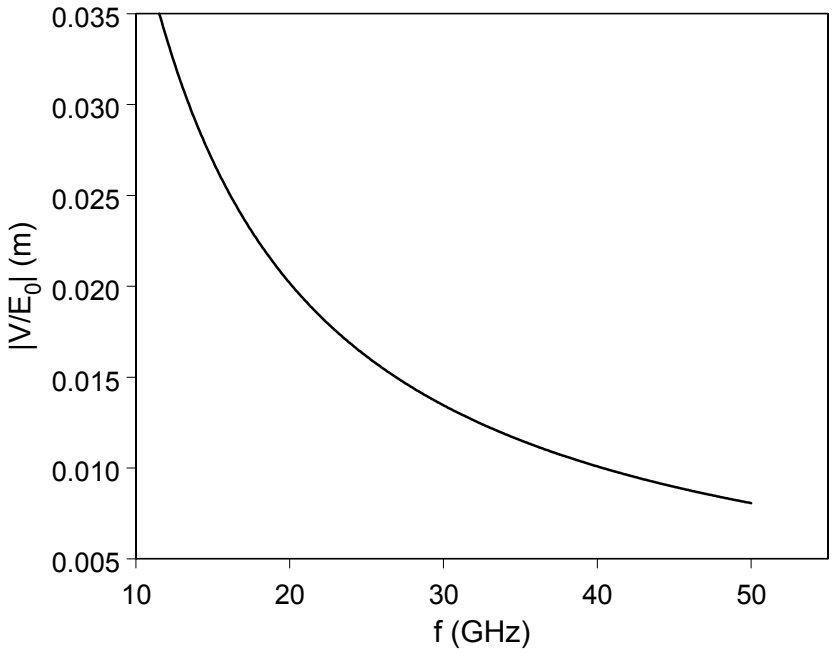

Figure 1: Ratio of voltage to electric field component (effective height) from bounding formula.

and at 40 GHz

$$|V(\ell)| \approx \frac{2Q}{k\ell} 2h_e E_0 \approx 0.010 \text{ m } E_0 \ , \ 40 \text{ GHz} \tag{54}$$

The plot of the ratio of the voltage to electric field component (effective height) in (52), using the fixed quality factor (51), is shown in Figure (1)

2.4 Random Plane Wave Drive

In an enclosed cavity environment at very high frequencies, the mean response should be estimated by averaging over the angle of incidence and the polarization angle. This would tend to reduce the coupling somewhat from the preceding maximum. If we take the transmission line to be oriented along the z unit vector $\underline{e}_z$, with the angle between the incident plane wavevector and the z axis again as θ_0, so again

$$\underline{k} \cdot \underline{r} = kx \sin\theta_0 \cos\varphi_0 + ky \sin\theta_0 \sin\varphi_0 + kz \cos\theta_0 \approx kz \cos\theta_0 \tag{55}$$

and having the unit vector $\underline{e}_x$ point between the wires from the negative to positive wire, with the voltage defined as

$$V = -\int_C \underline{E}^{ext} \cdot \underline{d\ell} \tag{56}$$

with the contour extending from the negative to the positive wire. In this section we now take the homogeneous case with wavenumber k.

Taking the field driving the line as the summation

$$\underline{E}^{ext}(\underline{r}) = E_0 \lim_{N\to\infty} \sqrt{2/N}\,\mathrm{Re}\left[\sum_{j=1}^{N} a_j \left(\cos\varphi_{pj}\underline{e}_j + \sin\varphi_{pj}\underline{e}'_j\right) e^{i\alpha_j + i\underline{k}_j\cdot\underline{r}}\right] \tag{57}$$

where the random amplitudes are normalized as

$$\langle a_j a_{j'}\rangle_{a_j} = \delta_{jj'} \tag{58}$$

which gives (with random phases α_j)

$$\left\langle \underline{E}^{ext}\cdot\underline{E}^{ext}\right\rangle_{a_j,\alpha_j} = E_0^2 \lim_{N\to\infty}\frac{2}{N}\sum_{j=1}^{N}\left\langle\cos^2\left(\alpha_j + \underline{k}_j\cdot\underline{r}\right)\right\rangle_{\alpha_j} = E_0^2 \tag{59}$$

The polarization angle φ_{pj} is a random function with orthogonal unit vector

$$\underline{e}'_j = \left(\underline{k}_j \times \underline{e}_j\right)/k \tag{60}$$

where

$$\underline{e}_j \cdot \underline{e}'_j = 0 \tag{61}$$

and the wavevectors are

$$\underline{k}_j = k\left(\underline{e}_x \sin\theta_j\cos\varphi_j + \underline{e}_y \sin\theta_j \sin\varphi_j + \underline{e}_z\cos\theta_j\right) \tag{62}$$

where

$$\underline{e}_j\cdot\underline{k}_j = 0 = \sin\theta_j\cos\varphi_j\sin\theta_{0j}\cos\varphi_{0j} + \sin\theta_j\sin\varphi_j\sin\theta_{0j}\sin\varphi_{0j} + \cos\theta_j\cos\theta_{0j}$$

$$= \sin\theta_j\sin\theta_{0j}\left(\cos\varphi_j\cos\varphi_{0j} + \sin\varphi_j\sin\varphi_{0j}\right) + \cos\theta_j\cos\theta_{0j}$$

$$= \sin\theta_j\sin\theta_{0j}\cos\left(\varphi_j - \varphi_{0j}\right) + \cos\theta_j\cos\theta_{0j} = \sin\theta_j\sin\theta_{0j}\left\{\cos\left(\varphi_j - \varphi_{0j}\right) - 1\right\} + \cos\left(\theta_j - \theta_{0j}\right) \tag{63}$$

If we have $\varphi_j - \varphi_{0j} = 0$ and $\theta_j - \theta_{0j} = \pm\pi/2$ this will vanish. This corresponds to taking the polarization vector $\underline{e}_j$ along a theta direction relative to the spherical radial direction for the wavevector. Taking $\theta_{0j} = \theta_j + \pi/2$ we can write

$$\underline{e}_j = \underline{e}_x\sin\theta_{0j}\cos\varphi_{0j} + \underline{e}_y\sin\theta_{0j}\sin\varphi_{0j} + \underline{e}_z\cos\theta_{0j}$$

$$= \underline{e}_x\cos\theta_j\cos\varphi_j + \underline{e}_y\cos\theta_j\sin\varphi_j - \underline{e}_z\sin\theta_j \tag{64}$$

and

$$\underline{e}'_j = \left(\underline{k}_j\times\underline{e}_j\right)/k$$

$$= \left(\underline{e}_x \sin\theta_j \cos\varphi_j + \underline{e}_y \sin\theta_j \sin\varphi_j + \underline{e}_z \cos\theta_j\right) \times \left(\underline{e}_x \sin\theta_{0j} \cos\varphi_{0j} + \underline{e}_y \sin\theta_{0j} \sin\varphi_{0j} + \underline{e}_z \cos\theta_{0j}\right)$$

$$= -\underline{e}_z \sin\left(\varphi_j - \varphi_{0j}\right) \sin\theta_j \sin\theta_{0j}$$

$$+\underline{e}_y \left(\cos\theta_j \sin\theta_{0j} \cos\varphi_{0j} - \sin\theta_j \cos\varphi_j \cos\theta_{0j}\right) + \underline{e}_x \left(\cos\theta_{0j} \sin\theta_j \sin\varphi_j - \cos\theta_j \sin\theta_{0j} \sin\varphi_{0j}\right)$$

$$= \underline{e}_y \left(\cos^2\theta_j + \sin^2\theta_j\right) \cos\varphi_j + \underline{e}_x \left(-\sin^2\theta_j - \cos^2\theta_j\right) \sin\varphi_j = \underline{e}_y \cos\varphi_j - \underline{e}_x \sin\varphi_j \tag{65}$$

The magnetic field can be found from Faraday's law

$$\nabla \times \underline{E} = i\omega\mu_0 \underline{H} \tag{66}$$

using

$$\underline{k}_j \times \underline{e}'_j = \underline{k}_j \times \left(\underline{k}_j \times \underline{e}_j\right)/k = -k\underline{e}_j \tag{67}$$

Noting that we can write

$$\underline{E}^{ext}(\underline{r}) = E_0 \lim_{N\to\infty} \sqrt{2/N}\frac{1}{2} \left[\sum_{j=1}^{N} a_j \left(\cos\varphi_{pj}\underline{e}_j + \sin\varphi_{pj}\underline{e}'_j\right)\left(e^{i\alpha_j + i\underline{k}_j\cdot\underline{r}} + e^{-i\alpha_j - i\underline{k}_j\cdot\underline{r}}\right)\right] \tag{68}$$

we find

$$\underline{H}^{ext}(\underline{r}) = \frac{kE_0}{i\omega\mu_0} \lim_{N\to\infty} \sqrt{2/N}\frac{1}{2} \left[\sum_{j=1}^{N} a_j \left(\cos\varphi_{pj}\underline{e}'_j - \sin\varphi_{pj}\underline{e}_j\right) i\left(e^{i\alpha_j + i\underline{k}_j\cdot\underline{r}} - e^{-i\alpha_j - i\underline{k}_j\cdot\underline{r}}\right)\right]$$

$$= \frac{kE_0}{\omega\mu_0} \lim_{N\to\infty} \sqrt{2/N}\frac{1}{2} \left[\sum_{j=1}^{N} a_j \left(\cos\varphi_{pj}\underline{e}'_j - \sin\varphi_{pj}\underline{e}_j\right)\left(e^{i\alpha_j + i\underline{k}_j\cdot\underline{r}} - e^{-i\alpha_j - i\underline{k}_j\cdot\underline{r}}\right)\right]$$

$$= -\frac{kE_0}{i\omega\mu_0} \lim_{N\to\infty} \sqrt{2/N}\,\mathrm{Im}\left[\sum_{j=1}^{N} a_j \left(\cos\varphi_{pj}\underline{e}'_j - \sin\varphi_{pj}\underline{e}_j\right) e^{i\alpha_j + i\underline{k}_j\cdot\underline{r}}\right]$$

$$= \frac{kE_0}{i\omega\mu_0} \lim_{N\to\infty} \sqrt{2/N}\,\mathrm{Re}\left[\sum_{j=1}^{N} a_j \left(\cos\varphi_{pj}\underline{e}'_j - \sin\varphi_{pj}\underline{e}_j\right)\left(ie^{i\alpha_j + i\underline{k}_j\cdot\underline{r}}\right)\right] \tag{69}$$

where

$$\frac{kE_0}{\omega\mu_0} = E_0/\eta_0 = H_0 \tag{70}$$

so that

$$\underline{H}^{ext}(\underline{r}) = -iH_0 \lim_{N\to\infty} \sqrt{2/N}\,\mathrm{Re}\left[\sum_{j=1}^{N} a_j \left(\cos\varphi_{pj}\underline{e}'_j - \sin\varphi_{pj}\underline{e}_j\right) ie^{i\alpha_j + i\underline{k}_j\cdot\underline{r}}\right] \tag{71}$$

and

$$H_\perp^{ext} = \underline{H}^{ext} \cdot \underline{e}_y = -iH_0 \lim_{N\to\infty} \sqrt{2/N}\,\mathrm{Re}\left[\sum_{j=1}^{N} a_j \left(\cos\varphi_{pj}\underline{e}'_j \cdot \underline{e}_y - \sin\varphi_{pj}\underline{e}_j \cdot \underline{e}_y\right) ie^{i\alpha_j + iz\underline{k}_j\cdot\underline{e}_z}\right]$$

$$= -iH_0 \lim_{N\to\infty} \sqrt{2/N}\,\mathrm{Re}\left[\sum_{j=1}^{N} a_j \left(\cos\varphi_{pj}\cos\varphi_j - \sin\varphi_{pj}\cos\theta_j\sin\varphi_j\right) ie^{i\alpha_j + ikz\cos\theta_j}\right] \tag{72}$$

This y component of the magnetic field (the component through the wires) must vanish when $\varphi_j = \pi/2$ with $\varphi_{pj} = 0$, because $\underline{H}^{ext}$ should then be x directed. Also we can write

$$E_\perp^{ext} = \underline{E}^{ext} \cdot \underline{e}_x = E_0 \lim_{N\to\infty} \sqrt{2/N}\,\mathrm{Re}\left[\sum_{j=1}^{N} a_j \left(\cos\varphi_{pj}\underline{e}_j \cdot \underline{e}_x + \sin\varphi_{pj}\underline{e}'_j \cdot \underline{e}_x\right) e^{i\alpha_j + iz\underline{k}_j\cdot\underline{e}_z}\right]$$

$$= E_0 \lim_{N\to\infty} \sqrt{2/N}\,\mathrm{Re}\left[\sum_{j=1}^{N} a_j \left(\cos\varphi_{pj}\cos\theta_j\cos\varphi_j - \sin\varphi_{pj}\sin\varphi_j\right) e^{i\alpha_j + ikz\cos\theta_j}\right] \tag{73}$$

The x component of the electric field (directed from wire to wire) must vanish when $\varphi_j = \pi/2$ with $\varphi_{pj} = 0$, because $\underline{E}^{ext}$ should then be in the $y-z$ plane.

Then the transmission line equations along the line are

$$\frac{dV}{dz} = -ZI - i\omega L^i H_\perp^{ext} \tag{74}$$

$$\frac{dI}{dz} + YV = i\omega C^i E_\perp^{ext} \tag{75}$$

or

$$\frac{d^2V}{dz^2} - ZYV = \left(\frac{d^2}{dz^2} + \Gamma^2\right) V = -i\omega L^i \frac{d}{dz} H_\perp^{ext} - i\omega C^i Z E_\perp^{ext}$$

$$= k\omega L^i H_0 \lim_{N\to\infty} \sqrt{2/N}\,\mathrm{Re}\left[\sum_{j=1}^{N} a_j \left(\cos\varphi_{pj}\cos\varphi_j - \sin\varphi_{pj}\cos\theta_j\sin\varphi_j\right) e^{i\alpha_j + ikz\cos\theta_j}\right]$$

$$= k\omega L^i H_0 \lim_{N\to\infty} \sqrt{2/N}\,\mathrm{Re}\left[\sum_{j=1}^{N} a_j \left(\cos\varphi_{pj}\cos\varphi_j - \sin\varphi_{pj}\cos\theta_j\sin\varphi_j\right)\cos\theta_j e^{i\alpha_j + ikz\cos\theta_j}\right]$$

$$-i\omega C^i Z E_0 \lim_{N\to\infty} \sqrt{2/N}\,\mathrm{Re}\left[\sum_{j=1}^{N} a_j \left(\cos\varphi_{pj}\cos\theta_j\cos\varphi_j - \sin\varphi_{pj}\sin\varphi_j\right) e^{i\alpha_j + ikz\cos\theta_j}\right] \tag{76}$$

Approximating $Z \approx -i\omega L$

$$\left(\frac{d^2}{dz^2} + \Gamma^2\right) V \approx \lim_{N\to\infty} \sqrt{2/N}\,\mathrm{Re}\left[\sum_{j=1}^{N} a_j \left\{k\omega L^i H_0 \left(\cos\varphi_{pj}\cos\varphi_j - \sin\varphi_{pj}\cos\theta_j\sin\varphi_j\right)\cos\theta_j\right.\right.$$

$$-\omega^2 C^i L E_0 \left(\cos\varphi_{pj}\cos\theta_j\cos\varphi_j - \sin\varphi_{pj}\sin\varphi_j\right)\Big\} e^{i\alpha_j + ikz\cos\theta_j}\Big]$$

$$\approx k\omega\mu_0 H_0 \lim_{N\to\infty}\sqrt{2/N}\,\mathrm{Re}\left[\sum_{j=1}^{N} a_j \Big\{\left(L^i/\mu_0\right)\left(\cos\varphi_{pj}\cos\varphi_j - \sin\varphi_{pj}\cos\theta_j\sin\varphi_j\right)\cos\theta_j\right.$$

$$\left. - \left(C^i/C\right)\left(\cos\varphi_{pj}\cos\theta_j\cos\varphi_j - \sin\varphi_{pj}\sin\varphi_j\right)\Big\} e^{i\alpha_j + ikz\cos\theta_j}\right] \tag{77}$$

Using

$$k^2 = \omega^2 LC \tag{78}$$

$$C^i/C = 2h_e \tag{79}$$

$$L^i/\mu_0 = 2h_e \tag{80}$$

we find

$$\left(\frac{d^2}{dz^2} + \Gamma^2\right) V \approx k2h_e\omega\mu_0 H_0 \lim_{N\to\infty}\sqrt{2/N}\,\mathrm{Re}\left[\sum_{j=1}^{N} a_j \sin^2\theta_j \sin\varphi_{pj}\sin\varphi_j e^{i\alpha_j + ikz\cos\theta_j}\right] \tag{81}$$

with solution

$$V = c_0\cos(\Gamma z) + c_1\sin(\Gamma z)$$

$$+k2h_e\omega\mu_0 H_0 \lim_{N\to\infty}\sqrt{2/N}\,\mathrm{Re}\left[\sum_{j=1}^{N} a_j \sin^2\theta_j \sin\varphi_{pj}\sin\varphi_j e^{i(\alpha_j + kz\cos\theta_j)}/\left(\Gamma^2 - k^2\cos^2\theta_j\right)\right] \tag{82}$$

as well as derivative

$$\frac{dV}{dz} = -ZI - i\omega L^i H_\perp^{ext}$$

$$-\Gamma c_0\sin(\Gamma z) + \Gamma c_1\cos(\Gamma z)$$

$$= -ZI - i\omega L^i H_0 \lim_{N\to\infty}\sqrt{2/N}\,\mathrm{Re}\left[\sum_{j=1}^{N} a_j \left(\cos\varphi_{pj}\cos\varphi_j - \sin\varphi_{pj}\cos\theta_j\sin\varphi_j\right) e^{i\alpha_j + ikz\cos\theta_j}\right]$$

$$+k2h_e\omega\mu_0 H_0 \lim_{N\to\infty}\sqrt{2/N}\,\mathrm{Im}\left[k\sum_{j=1}^{N} a_j \sin^2\theta_j \sin\varphi_{pj}\sin\varphi_j\cos\theta_j e^{i(\alpha_j + kz\cos\theta_j)}/\left(\Gamma^2 - k^2\cos^2\theta_j\right)\right] \tag{83}$$

If we take boundary conditions

$$V(0) = I(\ell) = 0 \tag{84}$$

we find

$$c_0 + k2h_e\omega\mu_0 H_0 \lim_{N\to\infty} \sqrt{2/N}\,\mathrm{Re}\left[\sum_{j=1}^{N} a_j \sin^2\theta_j \sin\varphi_{pj} \sin\varphi_j e^{i\alpha_j} / \left(\Gamma^2 - k^2\cos^2\theta_j\right)\right] = 0 \tag{85}$$

and

$$-\Gamma c_0 \sin(\Gamma\ell) + \Gamma c_1 \cos(\Gamma\ell)$$

$$= -i\omega L^i H_0 \lim_{N\to\infty} \sqrt{2/N}\,\mathrm{Re}\left[\sum_{j=1}^{N} a_j \left(\cos\varphi_{pj}\cos\varphi_j - \sin\varphi_{pj}\cos\theta_j\sin\varphi_j\right) e^{i\alpha_j + ik\ell\cos\theta_j}\right]$$

$$+k2h_e\omega\mu_0 H_0 \lim_{N\to\infty} \sqrt{2/N}\,\mathrm{Im}\left[k\sum_{j=1}^{N} a_j \sin^2\theta_j \sin\varphi_{pj}\sin\varphi_j\cos\theta_j e^{i(\alpha_j + k\ell\cos\theta_j)} / \left(\Gamma^2 - k^2\cos^2\theta_j\right)\right]$$

$$= \Gamma c_1 \cos(\Gamma\ell) + \Gamma\sin(\Gamma\ell)\, k2h_e\omega\mu_0 H_0 \lim_{N\to\infty} \sqrt{2/N}\,\mathrm{Re}\left[\sum_{j=1}^{N} a_j \sin^2\theta_j \sin\varphi_{pj}\sin\varphi_j e^{i\alpha_j} / \left(\Gamma^2 - k^2\cos^2\theta_j\right)\right]$$

$$= -i\omega L^i H_0 \lim_{N\to\infty} \sqrt{2/N}\,\mathrm{Re}\left[\sum_{j=1}^{N} a_j \left(\cos\varphi_{pj}\cos\varphi_j - \sin\varphi_{pj}\cos\theta_j\sin\varphi_j\right) e^{i\alpha_j + ik\ell\cos\theta_j}\right]$$

$$+k2h_e\omega\mu_0 H_0 \lim_{N\to\infty} \sqrt{2/N}\,\mathrm{Im}\left[k\sum_{j=1}^{N} a_j \sin^2\theta_j \sin\varphi_{pj}\sin\varphi_j\cos\theta_j e^{i(\alpha_j + k\ell\cos\theta_j)} / \left(\Gamma^2 - k^2\cos^2\theta_j\right)\right] \tag{86}$$

Then the voltage is

$$V(\ell) = c_0\cos(\Gamma\ell) + c_1\sin(\Gamma\ell)$$

$$+k2h_e\omega\mu_0 H_0 \lim_{N\to\infty} \sqrt{2/N}\,\mathrm{Re}\left[\sum_{j=1}^{N} a_j \sin^2\theta_j \sin\varphi_{pj}\sin\varphi_j e^{i(\alpha_j + kz\cos\theta_j)} / \left(\Gamma^2 - k^2\cos^2\theta_j\right)\right]$$

with

$$\Gamma = \sqrt{-ZY} = \Gamma' + i\Gamma'' \tag{87}$$

$$\Gamma'' \approx \frac{\Gamma'}{2}\left(\frac{R}{\omega L} + \frac{G}{\omega C}\right) = \frac{\Gamma'}{2}\left(1/Q_R + \tan\delta\right) = \Gamma'/(2Q) \tag{88}$$

$$\Gamma^2 - k^2\cos^2\theta_j \approx \Gamma'^2 + i2\Gamma'\Gamma'' - k^2\cos^2\theta_j \approx \Gamma'^2\left(1 + i/Q\right) - k^2\cos^2\theta_j \tag{89}$$

If there are no dielectric materials present (or a homogeneous region) $\Gamma' \approx k$

$$\Gamma^2 - k^2\cos^2\theta_j \approx k^2\left(\sin^2\theta_j + i/Q\right) \tag{90}$$

and

$$V(\ell) \approx c_0\cos(\Gamma\ell) + c_1\sin(\Gamma\ell)$$

$$+2h_e\frac{\omega\mu_0}{k}H_0\lim_{N\to\infty}\sqrt{2/N}\,\mathrm{Re}\left[\sum_{j=1}^{N}a_j\frac{\sin^2\theta_j}{\sin^2\theta_j + i/Q}\sin\varphi_{pj}\sin\varphi_j e^{i(\alpha_j + kz\cos\theta_j)}\right] \tag{91}$$

$$c_0 \approx -2h_e\frac{\omega\mu_0}{k}H_0\lim_{N\to\infty}\sqrt{2/N}\,\mathrm{Re}\left[\sum_{j=1}^{N}a_j\frac{\sin^2\theta_j}{\sin^2\theta_j + i/Q}\sin\varphi_{pj}\sin\varphi_j e^{i\alpha_j}\right] \tag{92}$$

$$\Gamma c_1\cos(\Gamma\ell) \approx -i\omega L^i H_0\lim_{N\to\infty}\sqrt{2/N}\,\mathrm{Re}\left[\sum_{j=1}^{N}a_j\left(\cos\varphi_{pj}\cos\varphi_j - \sin\varphi_{pj}\cos\theta_j\sin\varphi_j\right)e^{i\alpha_j + ik\ell\cos\theta_j}\right]$$

$$-2h_e\frac{\omega\mu_0}{k}H_0\lim_{N\to\infty}\sqrt{2/N}\,\mathrm{Re}\left[k\sum_{j=1}^{N}a_j\frac{\sin^2\theta_j}{\sin^2\theta_j + i/Q}\sin\varphi_{pj}\sin\varphi_j e^{i\alpha_j}\left\{\cos\theta_j ie^{ik\ell\cos\theta_j} + \frac{\Gamma}{k}\sin(\Gamma\ell)\right\}\right] \tag{93}$$

Using the approximation

$$\frac{\sin^2\theta_j}{\sin^2\theta_j + i/Q} \to 1 \quad , \quad \sin^2\theta_j >> 1/Q \tag{94}$$

$$V(\ell) \approx c_0\cos(\Gamma\ell) + c_1\sin(\Gamma\ell)$$

$$+2h_e\frac{\omega\mu_0}{k}H_0\lim_{N\to\infty}\sqrt{2/N}\,\mathrm{Re}\left[\sum_{j=1}^{N}a_j\sin\varphi_{pj}\sin\varphi_j e^{i(\alpha_j + k\ell\cos\theta_j)}\right] \tag{95}$$

$$c_0 \approx -2h_e\frac{\omega\mu_0}{k}H_0\lim_{N\to\infty}\sqrt{2/N}\,\mathrm{Re}\left[\sum_{j=1}^{N}a_j\sin\varphi_{pj}\sin\varphi_j e^{i\alpha_j}\right] \tag{96}$$

$$c_1\cos(\Gamma\ell) \approx -i2h_e\frac{\omega\mu_0}{k}H_0\lim_{N\to\infty}\sqrt{2/N}\,\mathrm{Re}\left[\sum_{j=1}^{N}a_j\left(\cos\varphi_{pj}\cos\varphi_j - \sin\varphi_{pj}\cos\theta_j\sin\varphi_j\right)e^{i\alpha_j + ik\ell\cos\theta_j}\right]$$

$$-2h_e\frac{\omega\mu_0}{k}H_0\lim_{N\to\infty}\sqrt{2/N}\,\mathrm{Re}\left[\sum_{j=1}^{N}a_j\sin\varphi_{pj}\sin\varphi_j\left\{\cos\theta_j ie^{i\alpha_j + ik\ell\cos\theta_j} + e^{i\alpha_j}\sin(k\ell)\right\}\right] \tag{97}$$

or

$$V(\ell) \approx c_0 \cos(\Gamma\ell) + c_1 \sin(\Gamma\ell)$$

$$+2h_e \frac{\omega\mu_0}{k} H_0 \lim_{N\to\infty} \sqrt{2/N} \left[\sum_{j=1}^{N} a_j \sin\varphi_{pj} \sin\varphi_j \cos(\alpha_j + k\ell\cos\theta_j) \right] \tag{98}$$

$$c_0 \approx -2h_e \frac{\omega\mu_0}{k} H_0 \lim_{N\to\infty} \sqrt{2/N} \left[\sum_{j=1}^{N} a_j \sin\varphi_{pj} \sin\varphi_j \cos(\alpha_j) \right] \tag{99}$$

$$c_1 \cos(\Gamma\ell) \approx -i2h_e \frac{\omega\mu_0}{k} H_0 \lim_{N\to\infty} \sqrt{2/N} \left[\sum_{j=1}^{N} a_j \left(\cos\varphi_{pj} \cos\varphi_j - \sin\varphi_{pj} \cos\theta_j \sin\varphi_j \right) \cos(\alpha_j + k\ell\cos\theta_j) \right]$$

$$-2h_e \frac{\omega\mu_0}{k} H_0 \lim_{N\to\infty} \sqrt{2/N} \left[\sum_{j=1}^{N} a_j \sin\varphi_{pj} \sin\varphi_j \left\{ -\cos\theta_j \sin(\alpha_j + k\ell\cos\theta_j) + \cos(\alpha_j) \sin(k\ell) \right\} \right] \tag{100}$$

Resonance occurs when $k\ell \to (n - 1/2)\,\pi$ and involves the $c_1 \sin(\Gamma\ell)$ voltage term through the $\cos(\Gamma\ell)$ factor

$$\cos(\Gamma\ell) \approx \cos(\Gamma'\ell) - i\Gamma''\ell \sin(\Gamma'\ell) \approx -i\Gamma''\ell\,(-1)^{n-1} = -i\,(-1)^{n-1}\,\Gamma'\ell/(2Q)$$

$$\approx -i\,(-1)^{n-1}\,k\ell/(2Q) \tag{101}$$

$$\sin(\Gamma\ell) \approx \sin(\Gamma'\ell) \approx \sin(k\ell) \approx (-1)^{n-1} \tag{102}$$

Taking the $c_1 \sin(\Gamma\ell)$ to be dominant

$$V(\ell) \approx c_1 \sin(\Gamma\ell)$$

$$\approx -i \tan(\Gamma\ell)\, 2h_e \frac{\omega\mu_0}{k} H_0 \lim_{N\to\infty} \sqrt{2/N} \left[\sum_{j=1}^{N} a_j \left(\cos\varphi_{pj} \cos\varphi_j - \sin\varphi_{pj} \cos\theta_j \sin\varphi_j \right) \cos(\alpha_j + k\ell\cos\theta_j) \right]$$

$$-\tan(\Gamma\ell)\, 2h_e \frac{\omega\mu_0}{k} H_0 \lim_{N\to\infty} \sqrt{2/N} \left[\sum_{j=1}^{N} a_j \sin\varphi_{pj} \sin\varphi_j \left\{ -\cos\theta_j \sin(\alpha_j + k\ell\cos\theta_j) + \cos(\alpha_j) \sin(k\ell) \right\} \right] \tag{103}$$

or

$$V(\ell)\, k\ell/(2Q) \approx 2h_e \frac{\omega\mu_0}{k} H_0 \lim_{N\to\infty} \sqrt{2/N}$$

$$\sum_{j=1}^{N} a_j \left\{ \cos\varphi_{pj} \cos\varphi_j \cos\left(\alpha_j + k\ell\cos\theta_j\right) - \sin\varphi_{pj} \sin\varphi_j \cos\theta_j e^{-i\left(\alpha_j + k\ell\cos\theta_j\right)} - i\sin\varphi_{pj} \sin\varphi_j \cos\left(\alpha_j\right)(-1)^{n-1} \right\} \tag{104}$$

If we average over incidence and polarization angles

$$\left\langle \left| V\left(\ell\right) k\ell/\left(2Q\right)\right|^2 \right\rangle = \frac{1}{4\pi}\int_0^{\pi} \sin\theta_j d\theta_j \int_0^{2\pi} d\varphi_j \frac{1}{2\pi}\int_0^{2\pi} \left\langle \left| V\left(\ell\right) k\ell/\left(2Q\right)\right|^2 \right\rangle_{a_j,\alpha_j} d\varphi_{pj}$$

$$\approx \left(2h_e \frac{\omega\mu_0}{k}\left|H_0\right|\right)^2 \frac{1}{4\pi}\int_0^{\pi} \sin\theta_j d\theta_j \int_0^{2\pi} d\varphi_j \frac{1}{2\pi}\int_0^{2\pi} d\varphi_{pj}\left(2/N\right)$$

$$\sum_{j=1}^{N}\sum_{j'=1}^{N} \left\langle a_j a_{j'} \right\rangle_{a_j} \left\langle \left\{ \cos\varphi_{pj} \cos\varphi_j \cos\left(\alpha_j + k\ell\cos\theta_j\right) - \sin\varphi_{pj} \sin\varphi_j \cos\theta_j e^{-i\left(\alpha_j + k\ell\cos\theta_j\right)} - i\sin\varphi_{pj} \sin\varphi_j \cos\left(\alpha_j\right)(-1)^{n-1} \right\} \right.$$

$$\left. \left\{ \cos\varphi_{pj'} \cos\varphi_{j'} \cos\left(\alpha_{j'} + k\ell\cos\theta_{j'}\right) - \sin\varphi_{pj'} \sin\varphi_{j'} \cos\theta_{j'} e^{i\left(\alpha_{j'} + k\ell\cos\theta_{j'}\right)} + i\sin\varphi_{pj'} \sin\varphi_{j'} \cos\left(\alpha_{j'}\right)(-1)^{n-1} \right\} \right\rangle_{\alpha_j}$$

$$\approx \left(2h_e \frac{\omega\mu_0}{k}\left|H_0\right|\right)^2 \frac{1}{4\pi}\int_0^{\pi} \sin\theta_j d\theta_j \int_0^{2\pi} d\varphi_j \frac{1}{2\pi}\int_0^{2\pi} d\varphi_{pj}\left(2/N\right)$$

$$\sum_{j=1}^{N} \left\langle \left\{ \cos\varphi_{pj} \cos\varphi_j \cos\left(\alpha_j + k\ell\cos\theta_j\right) - \sin\varphi_{pj} \sin\varphi_j \cos\theta_j e^{-i\left(\alpha_j + k\ell\cos\theta_j\right)} - i\sin\varphi_{pj} \sin\varphi_j \cos\left(\alpha_j\right)(-1)^{n-1} \right\} \right.$$

$$\left. \left\{ \cos\varphi_{pj} \cos\varphi_j \cos\left(\alpha_j + k\ell\cos\theta_j\right) - \sin\varphi_{pj} \sin\varphi_j \cos\theta_j e^{i\left(\alpha_j + k\ell\cos\theta_j\right)} + i\sin\varphi_{pj} \sin\varphi_j \cos\left(\alpha_j\right)(-1)^{n-1} \right\} \right\rangle_{\alpha_j}$$

$$\approx \left(2h_e \frac{\omega\mu_0}{k}\left|H_0\right|\right)^2 \frac{1}{4\pi}\int_0^{\pi} \sin\theta_j d\theta_j \int_0^{2\pi} d\varphi_j \frac{1}{2\pi}\int_0^{2\pi} d\varphi_{pj}\left(2/N\right)$$

$$\sum_{j=1}^{N} \left\langle \cos^2\varphi_{pj} \cos^2\varphi_j \cos^2\left(\alpha_j + k\ell\cos\theta_j\right) + \sin^2\varphi_{pj} \sin^2\varphi_j \cos^2\theta_j + \sin^2\varphi_{pj} \sin^2\varphi_j \cos^2\left(\alpha_j\right) \right.$$

$$- \cos\varphi_{pj} \cos\varphi_j \cos\left(\alpha_j + k\ell\cos\theta_j\right) \sin\varphi_{pj} \sin\varphi_j \cos\theta_j e^{i\left(\alpha_j + k\ell\cos\theta_j\right)}$$

$$+ \cos\varphi_{pj} \cos\varphi_j \cos\left(\alpha_j + k\ell\cos\theta_j\right) i\sin\varphi_{pj} \sin\varphi_j \cos\left(\alpha_j\right)(-1)^{n-1}$$

$$- \sin\varphi_{pj} \sin\varphi_j \cos\theta_j e^{-i\left(\alpha_j + k\ell\cos\theta_j\right)} \cos\varphi_{pj} \cos\varphi_j \cos\left(\alpha_j + k\ell\cos\theta_j\right)$$

$$- \sin\varphi_{pj} \sin\varphi_j \cos\theta_j e^{-i\left(\alpha_j + k\ell\cos\theta_j\right)} i\sin\varphi_{pj} \sin\varphi_j \cos\left(\alpha_j\right)(-1)^{n-1}$$

$$\left. -i\sin\varphi_{pj} \sin\varphi_j \cos\left(\alpha_j\right)(-1)^{n-1} \cos\varphi_{pj} \cos\varphi_j \cos\left(\alpha_j + k\ell\cos\theta_j\right) \right.$$

$$+i\sin\varphi_{pj}\sin\varphi_j\cos\left(\alpha_j\right)\left(-1\right)^{n-1}\sin\varphi_{pj}\sin\varphi_j\cos\theta_j e^{i(\alpha_j+k\ell\cos\theta_j)}\Big\rangle_{\alpha_j}$$

$$\approx\left(2h_e\frac{\omega\mu_0}{k}\left|H_0\right|\right)^2\frac{1}{4\pi}\int_0^{\pi}\sin\theta_j d\theta_j\int_0^{2\pi}d\varphi_j\frac{1}{2\pi}\int_0^{2\pi}d\varphi_{pj}\left(2/N\right)$$

$$\sum_{j=1}^{N}\left[\frac{1}{2}\cos^2\varphi_{pj}\cos^2\varphi_j+\sin^2\varphi_{pj}\sin^2\varphi_j\cos^2\theta_j+\frac{1}{2}\sin^2\varphi_{pj}\sin^2\varphi_j\right.$$

$$-\frac{1}{2}\cos\varphi_{pj}\cos\varphi_j\sin\varphi_{pj}\sin\varphi_j\cos\theta_j+\frac{i}{2}\cos\varphi_{pj}\cos\varphi_j\cos\left(k\ell\cos\theta_j\right)\sin\varphi_{pj}\sin\varphi_j\left(-1\right)^{n-1}$$

$$-\frac{1}{2}\sin\varphi_{pj}\sin\varphi_j\cos\theta_j\cos\varphi_{pj}\cos\varphi_j-\frac{i}{2}\sin^2\varphi_{pj}\sin^2\varphi_j\cos\theta_j\cos\left(k\ell\cos\theta_j\right)\left(-1\right)^{n-1}$$

$$-\frac{1}{2}\sin^2\varphi_{pj}\sin^2\varphi_j\cos\theta_j\sin\left(k\ell\cos\theta_j\right)\left(-1\right)^{n-1}-\frac{i}{2}\sin\varphi_{pj}\sin\varphi_j\left(-1\right)^{n-1}\cos\varphi_{pj}\cos\varphi_j\cos\left(k\ell\cos\theta_j\right)$$

$$\left.+\frac{i}{2}\sin^2\varphi_{pj}\sin^2\varphi_j\left(-1\right)^{n-1}\cos\theta_j\cos\left(k\ell\cos\theta_j\right)-\frac{i}{2}\sin^2\varphi_{pj}\sin^2\varphi_j\left(-1\right)^{n-1}\cos\theta_j\sin\left(k\ell\cos\theta_j\right)\right]$$

$$\approx\left(2h_e\frac{\omega\mu_0}{k}\left|H_0\right|\right)^2\frac{1}{2}\int_0^{\pi}\sin\theta_j d\theta_j\left(2/N\right)\frac{1}{8}\sum_{j=1}^{N}\left[2+2\cos^2\theta_j\right.$$

$$-i\cos\theta_j\cos\left(k\ell\cos\theta_j\right)\left(-1\right)^{n-1}-\cos\theta_j\sin\left(k\ell\cos\theta_j\right)\left(-1\right)^{n-1}$$

$$\left.+i\left(-1\right)^{n-1}\cos\theta_j\cos\left(k\ell\cos\theta_j\right)-i\left(-1\right)^{n-1}\cos\theta_j\sin\left(k\ell\cos\theta_j\right)\right]$$

$$\approx\left(2h_e\frac{\omega\mu_0}{k}\left|H_0\right|\right)^2\frac{1}{2}\int_{-1}^{1}du_j\left(2/N\right)\frac{1}{8}\sum_{j=1}^{N}\left[2+2u_j^2\right.$$

$$\left.-\left(1+i\right)u_j\sin\left(k\ell u_j\right)\left(-1\right)^{n-1}\right] \tag{105}$$

Using

$$\int u\sin\left(k\ell u\right)du=-\frac{u}{k\ell}\cos\left(k\ell u\right)+\frac{1}{\left(k\ell\right)^2}\sin\left(k\ell u\right) \tag{106}$$

we obtain

$$\left\langle\left|V\left(\ell\right)k\ell/\left(2Q\right)\right|^2\right\rangle\approx\left(2h_e\frac{\omega\mu_0}{k}\left|H_0\right|\right)^2\left(2/N\right)\frac{1}{8}\sum_{j=1}^{N}\int_0^{1}du_j\left[2+2u_j^2-\left(1+i\right)u_j\sin\left(k\ell u_j\right)\left(-1\right)^{n-1}\right]$$

$$\approx\left(2h_e\frac{\omega\mu_0}{k}\left|H_0\right|\right)^2\frac{2}{3}\left[1+\left(1+i\right)\left\{\cos\left(k\ell\right)-\frac{1}{\left(k\ell\right)}\sin\left(k\ell\right)\right\}\frac{3\left(-1\right)^{n-1}}{8k\ell}\right]\quad,\quad k\ell=\left(n-1/2\right)\pi \tag{107}$$

We note that at lower frequencies the second term is proportional to the first order spherical Bessel function

$$j_1(k\ell) = \frac{\sin(k\ell)}{(k\ell)^2} - \frac{\cos(k\ell)}{(k\ell)} \sim (k\ell)/3 \quad , \quad k\ell << 1 \tag{108}$$

and is therefore small in this limit. The leading term for high frequencies is

$$\sqrt{\left\langle |V(\ell)\, k\ell/(2Q)|^2 \right\rangle} \approx \left(2h_e \frac{\omega\mu_0}{k} |H_0|\right) \sqrt{\frac{2}{3}} \quad , \quad k\ell >> 1 \tag{109}$$

which is similar to the normal incidence maximum of the preceding section (except for the $\sqrt{2/3} \approx 0.8165$ factor); we note in this case that the squares of the electric and magnetic field amplitudes are the sum of the squares of the individual components

$$E_0^2 = E_{0x}^2 + E_{0y}^2 + E_{0z}^2 \tag{110}$$

$$H_0^2 = H_{0x}^2 + H_{0y}^2 + H_{0z}^2 \tag{111}$$

2.5 Rectangular Conductor Impedance/Loss Parameters

If the transmission line conductors are rectangular in cross section we can calculate the impedance per unit length using formulas for the equivalent radii of the rectangles and for the internal finitely conducting impedance per unit length (conductor losses).

The impedance per unit length is then written as

$$Z = R - iX = 2Z^{fi} - i\omega L_e \tag{112}$$

where for two equal width rectangular conductors of width $w = 2b$ and thickness $t = 2c$, separated by a sizable distance D compared to the equivalent radius a [7]

$$a/(w/4) \approx 1 + \frac{t}{\pi w}\left\{c_1 \ln(w/t) - \pi + \Gamma^2(1/4)/\sqrt{\pi}\right\} \tag{113}$$

for $t \leq w$ where $c_1 = 3/4$ and the gamma function $\Gamma(1/4) = 3.6256099$. Conveniently, t and w are interchanged for the case of $t > w$. The external inductance per unit length is again [3]

$$L_e = \frac{\mu_0}{\pi} \text{Arccosh}\left(\frac{D}{2a}\right) \sim \frac{\mu_0}{\pi} \ln(D/a) \ , \ D >> 2a \tag{114}$$

The finitely conducting internal impedance per unit length is [8], [9]

$$Z^{fi} \sim \frac{Z_s}{2\pi a_{loss}} + 4(A_0/I)^2 C_E$$

$$+ \left(\frac{Z_s}{2\pi a}\right)\left[\left(\frac{1}{2a}\right)\left(\frac{Z_s}{-i\omega\mu_0}\right) F(\kappa) + O\left(\left(\frac{1}{\gamma a}\right)^{4/3}, \left(\frac{Z_s}{-i\omega\mu_0 a}\right)^{4/3}\right)\right] \quad , \quad w, t >> \delta \tag{115}$$

where [7]

$$(w/2)/a_{loss} \approx 1 + \frac{1}{\pi}(1 - t/w)\ln(4\pi w/t)$$

$$-\frac{t}{\pi^2 w}\left[\ln\left(4\pi w/t\right)+\pi/2\right]\ln\left(w/t\right) \tag{116}$$

with corner corrections [9], [8]

$$C_E=-i\omega\mu\left(\frac{i}{\gamma}\right)^{4/3}\frac{2^{5/3}}{\sqrt{3}}D_c\left(\nu\right)=Z_s\left(\frac{i}{\gamma}\right)^{1/3}\frac{2^{5/3}}{\sqrt{3}}D_c\left(\nu\right) \tag{117}$$

with corner strength [9]

$$A_0/I=\frac{\kappa}{2\pi\left(3\kappa' C_1^2\right)^{1/3}}=\frac{1}{2\pi\left(12\kappa'\kappa a^2\right)^{1/3}} \tag{118}$$

where [7]

$$\left(t/w\right)/\left(\kappa\kappa'\right)^2\approx\frac{\pi}{4}\left[1+\frac{t}{\pi w}\left\{\ln\left(w/t\right)-\pi+\frac{16}{1+4/\pi}\right\}\right]\left(1+\frac{4t}{\pi w}\right) \tag{119}$$

and in the next term [7]

$$\left(t/w\right)F\left(\kappa\right)\approx\frac{1}{4\pi}+\frac{t}{4\pi^2 w}\left\{\ln\left(16w/t\right)\ln\left(w/t\right)-\pi+\frac{\Gamma^4\left(1/4\right)}{\pi}\right\} \tag{120}$$

In addition, the parameters $D_c\left(\nu\right)$, A_c, D_0, D_∞, and D_1 are given by [9]

$$D_c\left(\nu\right)\approx\frac{A_c D_0+D_\infty\nu^{15/12}}{A_c+\nu^{11/12}} \tag{121}$$

$$A_c=\frac{D_1-D_\infty}{D_0-D_1} \tag{122}$$

with

$$D_0=D_c\left(0\right)=\frac{\Gamma\left(1/3\right)}{2^{1/3}}\left[1-3\left\{\Gamma\left(2/3\right)/\Gamma\left(1/3\right)\right\}^3\right]\approx 1.30247 \tag{123}$$

$$D_\infty=\lim_{\nu\to\infty}\left[D_c\left(\nu\right)/\nu^{1/3}\right]=-\frac{3\pi^2 2^{1/3}}{4\Gamma^2\left(1/3\right)}\approx -1.29951 \tag{124}$$

and

$$D_1=D_c\left(1\right)\approx -0.360 \tag{125}$$

The leading term in (115) can often be used as an approximation.

The low frequency limit ($w,t<<\delta$) is [7]

$$Z^{fi}\sim R^{fi}-i\omega L^{fi}$$

where

$$R^{fi}=1/(2b2c\sigma) \tag{126}$$

and with $\mu=\mu_0$

$$L^{fi}\sim\frac{\mu_0}{2\pi}\ln(a)$$

$$-\frac{\mu_0}{2\pi}\left[\begin{array}{c}\ln\left(\sqrt{bc}\right)+\ln(2)-\frac{25}{12}+\frac{2}{3}\left\{\frac{b}{c}\text{Arctan}(\frac{c}{b})+\frac{c}{b}\text{Arctan}(\frac{b}{c})\right\}\\ +\frac{1}{4}\left\{(1-\frac{b^2}{3c^2})\ln(1+\frac{c^2}{b^2})+(1-\frac{c^2}{3b^2})\ln(1+\frac{b^2}{c^2})\right\}\end{array}\right] \tag{127}$$

2.5.1 Thin Strips

Electrically thin strips each of thickness $\Delta << w$ ($\delta >> \Delta/2$) have equivalent radius

$$a = b/2 = w/4 \tag{128}$$

and finitely conducting internal impedance per unit length Z^{fi} where [10], [11], [12]

$$\frac{\pi^2}{2}Z^{fi}/R_0 \sim 1+\ln\left(8\ell_{s0}b\right)+\gamma'-i\pi/2$$

$$+\frac{i}{2\pi\ell_{s0}b}\left\{\ln\left(8\ell_{s0}b\right)+\gamma'-i\pi/2\right\}^2 \quad , \quad 2\ell_{s0}b >> 1 \tag{129}$$

with

$$\ell_{s0} = \omega\mu_e\sigma\Delta/2 \tag{130}$$

and zero frequency resistance per unit length

$$R_0 = 1/\left(2b\sigma\Delta\right) = 1/\left(w\sigma\Delta\right) \tag{131}$$

with [10]

$$Z^{fi} \sim R_0 - i\frac{\omega\mu_0}{2\pi}\left[3/2-2\ln\left(2\right)\right] \quad , \quad 2\ell_{s0}b << 1 \tag{132}$$

2.5.2 Closely Spaced Strips

Two closely spaced strips of dimensions w, Δ a distance g apart, using planar approximations $g << w$, has impedance per unit length

$$Z = R - iX = 2Z^{fi} - i\omega L_e \tag{133}$$

with external inductance per unit length

$$L_e \sim \mu_0 g/\left(2b\right) = \mu_0 g/w \tag{134}$$

and internal impedance per unit length per strip with $\delta << \Delta/2$

$$Z^{fi} \sim Z_s/\left(2b\right) = Z_s/w \tag{135}$$

or with $\delta >> \Delta/2$

$$Z^{fi} \sim \left(\frac{1}{\sigma\Delta} - i\omega\mu\Delta/2\right)/w \tag{136}$$

2.5.3 Coplanar Thin Strips

From Smythe [13] the capacitance and external inductance per unit length between coplanar strips ($\Delta/2 >> \delta$) each of width $w = f - b$ and gap $g = 2b$ is

$$C/\varepsilon_0 = \frac{K(k')}{K(k)} = \mu_0/L_e \tag{137}$$

where

$$k = b/f \tag{138}$$

$$k' = \sqrt{1-k^2} \tag{139}$$

and the complete elliptic integral is defined by [14]

$$K(k) = \int_0^{\pi/2} d\theta/\sqrt{1-k^2\sin^2\theta} \tag{140}$$

There is a surprisingly accurate approximation for the ratio [15]

$$\frac{K(k')}{K(k)} \approx \frac{1}{\pi}\ln\left(2\frac{1+\sqrt{k'}}{1-\sqrt{k'}}\right) \tag{141}$$

If the strips are electrically thin ($\Delta/2 >> \delta$) and the gap is large $g > w$ we can take the internal impedance per unit length to be (129). Alternatively if the strips are electrically thick and the gap is large we can take the internal impedance per unit length to be (115).

2.6 Radiation Damping

We now briefly review the preceding radiation damping level for a resonant line with typical end conditions. For a line with two open circuited ends (open-open) we can write

$$P = \frac{1}{2}G_{rad}|V(0)|^2 + \frac{1}{2}G_{rad}|V(\ell)|^2 \tag{142}$$

where

$$\frac{dI}{dz} = i\omega CV \approx k_n I_0\cos(k_n z) = k_n I_0\cos\left(\frac{\pi n z}{\ell}\right) \tag{143}$$

and thus

$$V(0) = \frac{k_n}{i\omega C}I_0 = -iZ_c I_0 \tag{144}$$

$$V(\ell) = \frac{k_n}{i\omega C}I_0(-1)^n = -iZ_c I_0(-1)^n \tag{145}$$

or

$$P = Z_c^2 G_{rad}|I_0|^2 \tag{146}$$

Then we find [6]

$$G_{rad} = \frac{\omega\mu_0}{2\pi Z_c^2} k h_e^2 = \frac{\pi \left(k h_e\right)^2 / \eta}{2 \ln^2 \left(2h_e/a\right)} \ , \ k\ell \to n\pi \tag{147}$$

where the characteristic impedance is

$$Z_c = \frac{\eta}{\pi} \ln\left(2h_e/a\right) \ , \ \eta = \sqrt{\mu_0/\varepsilon'} \tag{148}$$

Alternatively, for two short circuited ends (short-short)

$$P = \frac{1}{2} R_{rad} \left|I\left(0\right)\right|^2 + \frac{1}{2} R_{rad} \left|I\left(\ell\right)\right|^2 = R_{rad} \left|I\left(0\right)\right|^2 \tag{149}$$

we find [6]

$$R_{rad} = \frac{\eta}{2\pi} \left(k h_e\right)^2 \ , \ k\ell \to n\pi \tag{150}$$

For an open-short combination (similar to the preceding section)

$$P = \frac{1}{2} G_{rad} \left|V\left(0\right)\right|^2 + \frac{1}{2} R_{rad} \left|I\left(\ell\right)\right|^2 \tag{151}$$

$$\frac{dI}{dz} = i\omega C V = k_n I\left(\ell\right) \cos\left(k_n z\right) \tag{152}$$

$$V\left(0\right) = \frac{k_n}{i\omega C} I\left(\ell\right) = -i Z_c I\left(\ell\right) \tag{153}$$

where [6]

$$G_{rad} Z_c^2 + R_{rad} = \frac{\eta}{\pi} \left(k h_e\right)^2 \tag{154}$$

We could alternatively place this perturbing radiation term exclusively at the shorted end, or exclusively at the open end, by setting the other term to zero. Note from the open-open and the short-short cases above we had

$$G_{rad} Z_c^2 = \eta \left(k h_e\right)^2 / \left(2\pi\right) = R_{rad} \tag{155}$$

2.7 Cascaded Transmission Systems

Electric field and voltage are not conserved quantities so an estimated level at each layer of the shield, as we often use with average power bounds in HERO analysis, does not apply to upset voltage levels. Instead, we have attempted to estimate maximum voltage levels coupled to cabling, and coupled to the input port of a component from measured effective height and impedance data, below. However, we really should verify that the transmission system from the component port to the sensitive device does not further boost such levels. (The third appendix also discusses the solution for a nonuniform line which could also be considered.)

In the analysis of the unshielded line we really would like to bound the response of two connected transmission lines, the first representing the driven cable section, and the second the interior component connection to the load of interest. What can we say about the voltage at the load end of the second line? Note that the second network may not have field coupling but be simply a connection between the ultimate load and the source cable.

Suppose we take two sections of transmission line hooked together to form the wire resonator. The right hand section has no drive field. We want to estimate a bound on the right-hand side voltage. We then require not only the open circuit voltage on the right hand side of the driven section, but also the impedance looking back into this driven section from this component port. This impedance is simply the input impedance of a section of line shorted at the opposite end. The new component section of line is taken to have impedance per unit length Z_1 and admittance per unit length Y_1 with a load Z_L at the right end. The ultimate load is transformed to the input impedance at the port between sections

$$Z_{i1} = Z_{01}\frac{Z_L\cos\left(\Gamma_1\ell_1\right) - iZ_{01}\sin\left(\Gamma_1\ell_1\right)}{Z_{01}\cos\left(\Gamma_1\ell_1\right) - iZ_L\sin\left(\Gamma_1\ell_1\right)} \tag{156}$$

The impedance on the left side of our assumed driven short-circuited line is

$$Z_i = -iZ_0\tan\left(\Gamma\ell\right) \tag{157}$$

The right section of line has transmission line equations

$$\frac{dV}{dz} = -Z_1 I \tag{158}$$

$$\frac{dI}{dz} = -Y_1 V \tag{159}$$

or eliminating the current

$$\left(\frac{d^2}{dz^2} + \Gamma_1^2\right)V = 0 \tag{160}$$

with propagation constant

$$\Gamma_1^2 = -Z_1 Y_1 \tag{161}$$

and characteristic impedance

$$Z_{01} = \sqrt{Z_1/Y_1} \tag{162}$$

We can write the voltage as

$$V\left(z\right) = c_{01}\cos\Gamma_1\left(z-\ell\right) + c_{11}\sin\Gamma_1\left(z-\ell\right) \tag{163}$$

At the new right load (the position of the vulnerable device) end of the second line the voltage is

$$V\left(\ell+\ell_1\right) = c_{01}\cos\left(\Gamma_1\ell_1\right) + c_{11}\sin\left(\Gamma_1\ell_1\right) = Z_L I\left(\ell+\ell_1\right) \tag{164}$$

with current

$$I\left(\ell+\ell_1\right) = \frac{\Gamma_1}{Z_1}\left[c_{01}\sin\left(\Gamma_1\ell_1\right) - c_{11}\cos\left(\Gamma_1\ell_1\right)\right] \tag{165}$$

so that

$$c_{01}\left\{\cos\left(\Gamma_1\ell_1\right) - \frac{Z_L}{Z_1}\Gamma_1\sin\left(\Gamma_1\ell_1\right)\right\} + c_{11}\left\{\sin\left(\Gamma_1\ell_1\right) + \frac{Z_L}{Z_1}\Gamma_1\cos\left(\Gamma_1\ell_1\right)\right\} = 0 \tag{166}$$

By current division at the left end of the new section of line

$$V(\ell+0) = c_{01} = V(\ell)\frac{Z_{i1}}{Z_i + Z_{i1}} \tag{167}$$

and therefore at the right load end voltage is

$$V(\ell+\ell_1) = V(\ell)\frac{Z_{i1}}{Z_i + Z_{i1}}\left[\cos(\Gamma_1\ell_1) + \frac{Z_L\Gamma_1\sin(\Gamma_1\ell_1) - Z_1\cos(\Gamma_1\ell_1)}{Z_1\sin(\Gamma_1\ell_1) + Z_L\Gamma_1\cos(\Gamma_1\ell_1)}\sin(\Gamma_1\ell_1)\right]$$

$$= V(\ell)\frac{Z_{i1}}{Z_i + Z_{i1}}\frac{Z_L}{(Z_1/\Gamma_1)\sin(\Gamma_1\ell_1) + Z_L\cos(\Gamma_1\ell_1)} \tag{168}$$

Using the new line characteristic impedance

$$Z_1/\Gamma_1 = Z_1/\left(\sqrt{-Z_1Y_1}\right) = -iZ_{01} \tag{169}$$

we can write this as

$$V(\ell+\ell_1) = V(\ell)\cos(\Gamma\ell)\frac{Z_{i1}}{(Z_i + Z_{i1})\cos(\Gamma\ell)}\frac{iZ_L}{Z_{01}\sin(\Gamma_1\ell_1) + iZ_L\cos(\Gamma_1\ell_1)} \tag{170}$$

where

$$Z_i\cos(\Gamma\ell) = -iZ_0\sin(\Gamma\ell) \tag{171}$$

$$V(\ell)\cos(\Gamma\ell) = -\sin(\Gamma\ell)\frac{L^i}{\mu_0}\frac{ik}{\Gamma}\eta_0 H_0 e^{ik\ell\cos\theta_0} \tag{172}$$

We see from these that the resonance $\Gamma'\ell = (n-1/2)\pi$, where $\cos(\Gamma'\ell) \to 0$, has been eliminated (as one would expect for the connected two-line system), and simply

$$V(\ell)\cos(\Gamma\ell) \to -(-1)^{n-1}\frac{L^i}{\mu_0}\frac{ik}{\Gamma}\eta_0 H_0 e^{ik\ell\cos\theta_0} \approx -(-1)^{n-1}\frac{ik}{\Gamma'}2h_e\eta_0 H_0 e^{ik\ell\cos\theta_0} \tag{173}$$

Furthermore, noting that

$$\frac{Z_{i1}}{(Z_i + Z_{i1})\cos(\Gamma\ell)}$$

$$= \frac{Z_{01}\left\{Z_L\cos(\Gamma_1\ell_1) - iZ_{01}\sin(\Gamma_1\ell_1)\right\}}{-iZ_0\left\{Z_{01}\cos(\Gamma_1\ell_1) - iZ_L\sin(\Gamma_1\ell_1)\right\}\sin(\Gamma\ell) + Z_{01}\left\{Z_L\cos(\Gamma_1\ell_1) - iZ_{01}\sin(\Gamma_1\ell_1)\right\}\cos(\Gamma\ell)} \tag{174}$$

the end voltage at the vulnerable component becomes

$$V(\ell+\ell_1) = V(\ell)\cos(\Gamma\ell)$$

$$\frac{Z_{01}Z_L}{-iZ_0\left\{Z_{01}\cos(\Gamma_1\ell_1) - iZ_L\sin(\Gamma_1\ell_1)\right\}\sin(\Gamma\ell) + Z_{01}\left\{Z_L\cos(\Gamma_1\ell_1) - iZ_{01}\sin(\Gamma_1\ell_1)\right\}\cos(\Gamma\ell)} \tag{175}$$

Obviously, if Z_L is of the same order as Z_0 any resonant enhancements are largely eliminated due to the damping of the load on the line. To introduce resonant behavior we need to take Z_L large (or small for

larger currents), or largely reactive (if we were to take it purely reactive, without losses, we would violate the spirit of having a load with a finite quality factor).

If we take a near open circuit at the terminals of interest $Z_L \to \infty$

$$V(\ell+\ell_1) = V(\ell)\cos(\Gamma\ell)\frac{Z_{01}}{-Z_0\sin(\Gamma_1\ell_1)\sin(\Gamma\ell)+Z_{01}\cos(\Gamma_1\ell_1)\cos(\Gamma\ell)} \tag{176}$$

Using some trigonometric identities

$$V(\ell+\ell_1) = V(\ell)\cos(\Gamma\ell)\frac{2Z_{01}}{(Z_{01}-Z_0)\cos(\Gamma\ell-\Gamma_1\ell_1)+(Z_{01}+Z_0)\cos(\Gamma\ell+\Gamma_1\ell_1)} \tag{177}$$

Introducing real and imaginary parts of the propagation constant (where the imaginary part is again taken as a small perturbation)

$$\Gamma\ell \pm \Gamma_1\ell_1 = (\Gamma'\ell \pm \Gamma_1'\ell_1) + i(\Gamma''\ell \pm \Gamma_1''\ell_1) \tag{178}$$

we see that resonance is produced when

$$(Z_{01}-Z_0)\cos(\Gamma'\ell-\Gamma_1'\ell_1)+(Z_{01}+Z_0)\cos(\Gamma'\ell+\Gamma_1'\ell_1) = 0 \tag{179}$$

in which case

$$V(\ell+\ell_1) = V(\ell)\cos(\Gamma\ell)$$

$$\frac{i2Z_{01}}{(Z_{01}-Z_0)((\Gamma''\ell-\Gamma_1''\ell_1))\sin(\Gamma'\ell-\Gamma_1'\ell_1)+(Z_{01}+Z_0)((\Gamma''\ell+\Gamma_1''\ell_1))\sin(\Gamma'\ell+\Gamma_1'\ell_1)} \tag{180}$$

For equal characteristic impedances $Z_{01} = Z_0$ this becomes

$$V(\ell+\ell_1) = \frac{V(\ell)\cos(\Gamma\ell)}{\cos(\Gamma\ell+\Gamma_1\ell_1)} \tag{181}$$

and at resonance $\Gamma'\ell+\Gamma_1'\ell_1 = (n-1/2)\pi$

$$\cos(\Gamma'\ell+\Gamma_1'\ell_1) = 0 \tag{182}$$

we obtain

$$\frac{V(\ell+\ell_1)}{V(\ell)\cos(\Gamma\ell)} \approx \frac{i(-1)^{n-1}V(\ell+\ell_1)}{(k/\Gamma')2h_e\eta_0 H_0 e^{ik\ell\cos\theta_0}} \approx \frac{i(-1)^{n-1}}{\Gamma''\ell+\Gamma_1''\ell_1} \tag{183}$$

Thus in this matched case (equal characteristic impedances) we simply replace $\Gamma''\ell$ by $\Gamma''\ell+\Gamma_1''\ell_1$ and the resonant enhancement of the voltage is decreased relative to the single driven cable. Because we do not expect significant changes in characteristic impedance along the line, we do not see the change from the single line to this cascaded system as introducing any increases in the maximum voltage.

As a second example, if we take a factor of two change in characteristic impedance $Z_{01} = 2Z_0$ or $Z_0 = 2Z_{01}$, then the resonance condition (179) becomes

$$\pm\frac{1}{3}\cos(\Gamma'\ell-\Gamma_1'\ell_1)+\cos(\Gamma'\ell+\Gamma_1'\ell_1) = 0 \tag{184}$$

where the upper sign corresponds to $Z_{01} = 2Z_0$ and the lower sign corresponds to $Z_0 = 2Z_{01}$. Thus bounding the magnitude of the first trigonometric function by unity gives

$$\left|\cos\left(\Gamma'\ell+\Gamma'_1\ell_1\right)\right|<1/3 \tag{185}$$

and through $|\sin x|=\sqrt{1-\cos^2 x}$ we can write

$$\left|\sin\left(\Gamma'\ell+\Gamma'_1\ell_1\right)\right|>\sqrt{1-1/3^2}>0.943 \tag{186}$$

Then from (180) we obtain

$$V\left(\ell+\ell_1\right)=V\left(\ell\right)\cos\left(\Gamma\ell\right)\frac{i}{\left(\Gamma''\ell-\Gamma''_1\ell_1\right)\sin\left(\Gamma'\ell-\Gamma'_1\ell_1\right)+\frac{3}{2}\left(\Gamma''\ell+\Gamma''_1\ell_1\right)\sin\left(\Gamma'\ell+\Gamma'_1\ell_1\right)} \tag{187}$$

and

$$V\left(\ell+\ell_1\right)=V\left(\ell\right)\cos\left(\Gamma\ell\right)\frac{i}{-\frac{1}{2}\left(\Gamma''\ell-\Gamma''_1\ell_1\right)\sin\left(\Gamma'\ell-\Gamma'_1\ell_1\right)+\frac{3}{2}\left(\Gamma''\ell+\Gamma''_1\ell_1\right)\sin\left(\Gamma'\ell+\Gamma'_1\ell_1\right)} \tag{188}$$

Using these prior bounding results, and further bounding the first trigonometric functions in the denominator by unity, these can be re-written as

$$\left|\frac{V\left(\ell+\ell_1\right)}{V\left(\ell\right)\cos\left(\Gamma\ell\right)}\right|\approx\left|\frac{1}{\left(\Gamma''\ell-\Gamma''_1\ell_1\right)\pm\frac{3}{2}\left(\Gamma''\ell+\Gamma''_1\ell_1\right)0.943}\right|<\left|\frac{1}{0.4145\Gamma''\ell+2.4145\Gamma''_1\ell_1}\right|,\left|\frac{1}{2.4145\Gamma''\ell+0.4145\Gamma''_1\ell_1}\right| \tag{189}$$

and

$$\left|\frac{V\left(\ell+\ell_1\right)}{V\left(\ell\right)\cos\left(\Gamma\ell\right)}\right|\approx\left|\frac{1}{-\frac{1}{2}\left(\Gamma''\ell-\Gamma''_1\ell_1\right)\pm\frac{3}{2}\left(\Gamma''\ell+\Gamma''_1\ell_1\right)0.943}\right|<\left|\frac{1}{0.9145\Gamma''\ell+1.9145\Gamma''_1\ell_1}\right|,\left|\frac{1}{1.9145\Gamma''\ell+0.9145\Gamma''_1\ell_1}\right| \tag{190}$$

Suppose, as another example $Z_0=3Z_{01}$ (note that for $Z_0=100$ ohms, $Z_0=3Z_{01}$ corresponds to $Z_{01}=33.3$ ohms, and $Z_{01}=2Z_0$ corresponds to $Z_{01}=200$ ohms), then the resonance condition becomes

$$-\frac{1}{2}\cos\left(\Gamma'\ell-\Gamma'_1\ell_1\right)+\cos\left(\Gamma'\ell+\Gamma'_1\ell_1\right)=0 \tag{191}$$

Bounding

$$\left|\cos\left(\Gamma'\ell+\Gamma'_1\ell_1\right)\right|<1/2 \tag{192}$$

$$\left|\sin\left(\Gamma'\ell+\Gamma'_1\ell_1\right)\right|>\sqrt{1-1/2^2}>0.866 \tag{193}$$

and applying these gives

$$V\left(\ell+\ell_1\right)=V\left(\ell\right)\cos\left(\Gamma\ell\right)\frac{i}{-\left(\Gamma''\ell-\Gamma''_1\ell_1\right)\sin\left(\Gamma'\ell-\Gamma'_1\ell_1\right)+2\left(\Gamma''\ell+\Gamma''_1\ell_1\right)\sin\left(\Gamma'\ell+\Gamma'_1\ell_1\right)} \tag{194}$$

and

$$\left|\frac{V(\ell+\ell_1)}{V(\ell)\cos(\Gamma\ell)}\right| \approx \left|\frac{1}{-(\Gamma''\ell-\Gamma_1''\ell_1)\pm 2(\Gamma''\ell+\Gamma_1''\ell_1)\,0.866}\right| < \left|\frac{1}{0.732\Gamma''\ell+2.732\Gamma_1''\ell_1}\right|, \left|\frac{1}{2.732\Gamma''\ell+0.732\Gamma_1''\ell_1}\right| \tag{195}$$

Our prior result with the driven cable

$$\left|\frac{V(\ell)}{2h_e\eta_0 H_0}\right| \approx \frac{1}{\Gamma''\ell} \approx \frac{2Q}{k\ell} \tag{196}$$

compared with these cascaded results, indicates that for the matched case $Z_{01}=Z_0$, because $\Gamma''\ell+\Gamma_1''\ell_1 > \Gamma''\ell$, we obtain a smaller voltage result. Furthermore, if we have $Z_{01}=Z_0/2$ with $0.9145\Gamma''\ell+1.9145\Gamma_1''\ell_1 > \Gamma''\ell$ and for $Z_{01}=Z_0/3$ with $0.732\Gamma''\ell+2.732\Gamma_1''\ell_1 > \Gamma''\ell$ then we also obtain smaller voltage results. Finally, for $Z_{01}=2Z_0$, if $0.4145\Gamma''\ell+2.4145\Gamma_1''\ell_1 > \Gamma''\ell$ we also obtain a smaller voltage result. This indicates, that we will usually obtain smaller voltages for the lossy cascaded system (at least for a restricted range of characteristic impedances).

Characteristic impedances from 33.3 ohms to 200 ohms cover a wide range of practical transmission lines. For example, a microstrip line (single trace) on FR4 dielectric ($\varepsilon_r=4.4$), 1 oz. copper traces ($t=1.4$ mils), and a typical substrate thickness of 0.125 inches would require a trace width of 0.44 inches to have a characteristic impedance of 33.3 ohms. The same structure would achieve a characteristic impedance of 198 ohms with a trace width of 0.0025 inches.

2.8 Experimental Effective Height Approach

Measurements of the effective height of the pins in a cable are sometimes made up to 40 GHz; measurements of the effective height of the pins in a canonical Belden 8240 cable have also been made up to 20 GHz. The source at the end of the cable has open circuit voltage V_{oc} (extrapolated by using the voltage into the 50 ohm measurement system and the corresponding measured source impedance $Z_{src}=R_{src}-iX_{src}$ converted to time dependence $e^{-i\omega t}$). This measured source feeds the component port (the second transmission line, above). If we take the component port impedance to be Z_p then the voltage at this port is

$$V_p = \frac{Z_p}{Z_{src}+Z_p}V_{oc} \tag{197}$$

We often do not really know the port impedance Z_p. If we adjust it to maximize the port voltage V_p we can take

$$Z_p = \mathrm{Im}(Z_{src}^*) \tag{198}$$

(this purely reactive choice is extreme in that we have ignored losses in the component line and load, but often the measured data from the driven cable allows us to get away with this extreme bounding choice) in which case

$$V_p = \frac{\mathrm{Im}(Z_{src}^*)}{\mathrm{Re}(Z_{src})}V_{oc} = \frac{X_{src}}{R_{src}}V_{oc} \tag{199}$$

If we define a source quality factor as the limiting value

$$\frac{|X_{src}|}{R_{src}} \le Q_{src} \tag{200}$$

we see that such port loads can magnify the port voltage over the open circuit level

$$|V_p| \leq Q_{src} \, |V_{oc}| \tag{201}$$

We should note here that the adaptors used in the effective height measurements introduce major perturbations into the results relative to what would be found if measurements could be made without them. We hope that extremes in wideband spectral responses are somewhat insensitive to the large reactances introduced, but the bulk measurements obviously affect the real impedance levels as well (for example, the characteristic impedance becomes the bulk level versus an individual wire level). Experimental results may end up being lower than our analytical result (52), which could be due to cable shielding (adaptor & bulk effects may also play some role) and could also be due to nearly overlapping TEM cable modes in the experimental measurements.

This page left blank

3 POWER COUPLING AND HERO

We have flexibility for what we choose as a worst case model for Hazard of Electromagnetic Radiation to Ordnance (HERO) assessment. Since hot-wire electro-explosive initiators have substantial thermal time constants, which would average over the pulse repetition period of a modulated incident pulse train, one approach would be to begin by using the exterior "average" field level exposure (where average fields are defined to deliver the same time average power density as the modulated pulse train). Armed with the fact that steady-state power is conserved in a passive system, we first make use of power bounds for apertures [16], [17], [18] in the exterior conducting barrier to bound the received level at electro-explosive devices within. For example the transmitted power through the aperture can be estimated as

$$P_{trans} = \sigma_{trans}^{Deep} S^{inc} \tag{202}$$

with incident power density

$$S^{inc} = \left|\underline{E}^{inc}\right|^2 / \eta_0 \tag{203}$$

and the slot cross section will be discussed in the next section.

If it is necessary to reduce these power estimates further, we next proceed inward to the cables and finally to the pins. In the remainder of this section we will use estimates of the interior cavity field levels in the next section to estimate bounds on antenna/cable pickup on the interior.

3.1 Matched Dipole Antenna

It has become traditional to use a simple matched antenna model to bound cable pickup in assembly areas [19]. This antenna is usually taken as a simple dipole. It is assumed that the intervening cabling from a low impedance electro-explosive device load is able to transform the impedance into a matching impedance at the antenna interface. Hence, through conservation of power, the power received at the matched antenna is taken as a bound on that delivered to the electro-explosive device. We can write this as

$$P_{rec} = A_e S^{inc} \tag{204}$$

where for root mean square (rms) units we can take the incident power density to be

$$\underline{S}^{inc} = \underline{E}^{inc} \times \underline{H}^{inc} \tag{205}$$

The effective area is [20]

$$A_e = \frac{\lambda^2}{4\pi} G p q \tag{206}$$

where G is the directivity gain, $0 \leq p \leq 1$ is the polarization mismatch factor, which for a wire antenna aligned with the z axis

$$p = \left(\underline{e}_\theta \cdot \underline{E}^{inc}\right)^2 / \left|\underline{E}^{inc}\right|^2 \tag{207}$$

and $0 \leq q \leq 1$ is the circuit mismatch factor (for the matched case this is set to unity)

$$q = \frac{4 \operatorname{Re}(Z_L) \operatorname{Re}(Z_{ant})}{|Z_L + Z_{ant}|^2} \tag{208}$$

The average over the polarization gives

$$\langle p \rangle = 1/2 \tag{209}$$

and the average over the incident angles gives

$$\langle G \rangle = 1 \tag{210}$$

The received power when averaged over all incident angles and polarization (as in an overmoded cavity) is then

$$\langle P_{rec} \rangle = \frac{\lambda^2}{8\pi} S \tag{211}$$

where the average power density in the cavity volume V can be written as

$$S = \left\langle |\underline{E}|^2 \right\rangle_V / \eta_0 = 3 \left\langle |E_i|^2 \right\rangle_V / \eta_0 = \eta_0 \left\langle |\underline{H}|^2 \right\rangle_V = 3\eta_0 \left\langle |H_i|^2 \right\rangle_V \tag{212}$$

with free space impedance

$$\eta_0 = \sqrt{\mu_0/\varepsilon_0} \approx 120\pi \text{ ohms} \tag{213}$$

and where the electric field is $\underline{E}$ with components E_i , $i = 1, 2, 3$ and the magnetic field is $\underline{H}$ with components H_i , $i = 1, 2, 3$. Note that on the conducting boundary A of the cavity there is a 3 dB field enhancement for the nonzero components $2 \left\langle |H_i|^2 \right\rangle_V = \left\langle |H_j|^2 \right\rangle_A$, $j = 1, 2$ and $2 \left\langle |E_i|^2 \right\rangle_V = \left\langle |E_n|^2 \right\rangle_A$, where j denotes the two tangential components and n denotes the normal component. Then

$$P_{rec} = \frac{\lambda^2}{8\pi} S = \frac{\lambda^2}{8\pi} \left\langle |\underline{E}|^2 \right\rangle_V / \eta_0 = \frac{\lambda^2}{4\pi} \frac{3}{2} \left\langle |E_i|^2 \right\rangle_V / \eta_0 \tag{214}$$

There are fluctuations about these average responses [19]. However, we note that because there is a high degree of modal overlap in the three-dimensional cavity at the higher end of the frequency range [21] (typically, say $10 - 50$ GHz), in this range we can write

$$\alpha = \frac{k_0^3 V}{2\pi Q_{cav}} >> 1 \tag{215}$$

where

$$k_0 = \omega\sqrt{\mu_0 \varepsilon_0} \tag{216}$$

and the antenna will respond approximately as if it is in free space; we use the zero subscript to denote the free space value and k for propagation in the dielectric materials (otherwise we simply use k for free space when materials are not present). Consequently, the fluctuations of a resonant dipole would result from the field variations within the cavity, which are taken to be bounded by the extreme field E_i selected in the subsection below.

The directivity gain of a small electric dipole in free space is

$$G_{smdip} = 3/2 \tag{217}$$

so that for an incident plane wave field in free space with aligned polarization $p = 1$ and matched load ($q = 1$)

$$P_{rec} = \frac{\lambda^2}{4\pi} G_{smdip} pq \left| E_i \right|^2 / \eta_0 = \frac{\lambda^2}{4\pi} \frac{3}{2} \left| E_i \right|^2 / \eta_0 \tag{218}$$

For a small resonant dipole (first resonance) in free space this gain increases only slightly from the short limit to

$$G_{resdip} = 1.64 \tag{219}$$

and the traditional formula used in the "V-curve" is

$$P_{rec} = \frac{\lambda^2}{4\pi} G_{resdip} \left|E_i\right|^2 / \eta_0 = \frac{\lambda^2}{4\pi} 1.64 \left|E_i\right|^2 / \eta_0 \tag{220}$$

These traditional values, which are only slightly larger than what is expected for the cavity response (214), are given in the next subsection.

This page left blank

4 EXAMPLE VOLTAGE AND POWER RESULTS

The exterior field drives from the Military Standards are used to drive the preceding results.

4.1 Exterior And Interior Field Example

Electromagnetic radiation (EMR) field descriptions can be found in the Military Standards [22]. The worst case is typically the table for shipboard emissions. In this case we use some simple rounded levels in the high frequency region, say above 5 GHz, [22] and take the peak level as

$$E_{peak} \approx 3 \text{ kV/m-rms} \tag{221}$$

and the corresponding average level as

$$E_{ave} \approx 0.6 \text{ kV/m-rms} \tag{222}$$

In the first appendix we take an example with a slot length $\ell = 2h \approx 2$ in, slot depth $d \approx 0.5$ in, slot width $w = 0.002$ in, aluminum slot and cavity walls with $\mu = \mu_0$, $\sigma \approx 2.6 \times 10^7$ S/m, and cavity area $A \approx 0.5$ m^2. Evaluation at $f = 25 - 50$ GHz gives (using the preceding Deep slot formulas) gives the mean interior field single component fields

$$\left\langle |H_i|^2 \right\rangle / \left|H_0^{inc}\right|^2 \approx 0.0864 - 0.0475 \, (-10.6 \text{ to } -13.2 \text{ dB}) \approx \left\langle |E_i|^2 \right\rangle / \left|E_0^{inc}\right|^2 \tag{223}$$

and using the overmoded distribution in the first appendix

$$|E_i|^2 / \left|E_0^{inc}\right|^2 \leq 3 \left\langle |E_i|^2 \right\rangle / \left|E_0^{inc}\right|^2 \approx 0.2593 - 0.1425 \, (-5.9 \text{ to } -8.5 \text{ dB}) \text{ , 95\% confidence} \tag{224}$$

If we assume the modulated pulse is long compared to the cavity quality factor times the carrier period, at the 95% level the interior single component peak field is

$$\left|E_i^{peak}\right| \approx 1.5 - 1.1 \text{ kV/m-rms} \tag{225}$$

and the average interior single component field at the 95% level is

$$|E_i^{ave}| \approx 0.31 - 0.23 \text{ kV/m-rms} \tag{226}$$

4.2 Unshielded Cable Voltages

If we take a typical minimum cable length of $\ell = 12$ inches, a wire-to-wire spacing $D \approx 0.06$ inches with $2a \approx 0.032$ inches, 25 GHz frequency,and a quality factor $Q \leq 1000$ due to a combination of absorptive losses, we see that a differential mode will have a port voltage over the range $25 - 50$ GHz

$$|V(\ell)/E_i| \approx \frac{2Q}{k\ell} 2h_e \approx 0.016 - 0.008 \text{ m} \tag{227}$$

The coupled voltage to an unshielded cable using the 95% maximum peak interior field

$$\left|E_i^{peak}\right| \approx 1.5 - 1.1 \text{ kV/m-rms} \tag{228}$$

is then

$$|V(\ell)| \approx 24 - 8.8 \text{ volts} \tag{229}$$

4.3 Slot Transmitted Power

From the first appendix the Deep slot transmitted power is

$$P_{trans} = \sigma_{trans}^{Deep} S^{inc} \tag{230}$$

with incident power density

$$S^{inc} = \left|\underline{E}^{inc}\right|^2 / \eta_0 \tag{231}$$

The first appendix gives the Deep slot cross section for $f = 25 - 50$ GHz

$$\sigma_{trans}^{Deep} \approx \frac{\lambda \ell}{\pi} p_{slot} q_{trans}^{Deep} \leq 3.0148 - 2.2277 \times 10^{-5} \text{ m}^2 \tag{232}$$

Using the exterior average field

$$E_{ave} \approx 0.6 \text{ kV/m-rms} \tag{233}$$

this gives

$$P_{trans} = 29 - 21 \text{ mW} \tag{234}$$

4.4 Antenna Power Results

The V-curve matched dipole bound to the power that could be delivered to an electro-explosive device is

$$P_{rec} = \frac{\lambda^2}{4\pi} G_{resdip} \left|E_i\right|^2 / \eta_0 = \frac{\lambda^2}{4\pi} 1.64 \left|E_i\right|^2 / \eta_0 \tag{235}$$

Using the 95% maximum average interior field

$$|E_i^{ave}| \approx 0.31 - 0.23 \text{ kV/m-rms} \tag{236}$$

then gives the received power over the $f = 25 - 50$ GHz range

$$P_{rec} \approx 4.8 - 0.66 \text{ mW} \tag{237}$$

5 COMPONENT SCREENING LEVELS

The hot-wire ordnance thresholds are taken as a no-fire power level. For the most common hot-wire electro-explosive devices the no-fire power threshold is one Watt

$$P_{nf} = 1 \text{ W} \tag{238}$$

Typically, the calculations for initiation of hot wire devices use the exterior average field, relying on the size of the thermal time constant of such devices being longer than the pulse repetition time. The preceding estimates for the coupled power at the ordnance were very small compared to this level. Frequently, a significant margin is also required to arrive at a screening power level for ordnance; the preceding received power levels were sufficiently small compared to this threshold they would afford more than enough margin.

The upset thresholds are taken as a voltage level for typical logic circuits. Because the high frequencies being considered here for the electromagnetic radiation may be quite different from the operating frequency spectrum of the electronic system, interference with the system operation may require rectification of the electromagnetic radiation induced voltages in order to effectively disrupt operation. Although this may result in substantial increases in the required threshold voltages for upset, without detailed information on this increase in level, we will assume a conservative screening level of

$$V_{up} = 1 \text{ V-rms} \tag{239}$$

Note that this choice of voltage screening level was assumed from five volt logic voltage thresholds at normal operating frequencies. Because, this screening level should be smaller than the actual threshold (particularly at much higher frequencies, which would likely require a nonlinear demodulation mechanism-rectification), and required margins for upset reliability are typically smaller than those for ordnance safety, this bounding analysis should also cover pulse train modulated drives (because we are using the peak drive field level). However, the preceding voltage estimates for the unshielded cable are above this conservative screening level. Nevertheless, an interior shielded cable will often provide an additional reduction of twenty to forty dB or more, which would bring the preceding estimated levels to the range of or below this screening voltage.

This page left blank

6 CONCLUSIONS

Bounding models are discussed for field coupling to an unshielded cable at resonances. Estimates for the resonant quality factor which include both conductor and dielectric losses (as well as radiation) are made and used in the response. Although maximum plane wave arrangements are used we also compare this to an average over incident and polarization angles more representative of an interior cavity field. The appendices also briefly discuss the case of a shielded cable.

The matched load approach used in the construction of the V-curve is discussed to bound received power when ordnance is being considered.

An example is given of a slot in an enclosure, with power balance being used to estimate the interior field levels given exterior field drives from the military standards (transmitted power through a slot in the enclosure barrier is also given). The interior field level is estimated in the canonical shield and cavity for the $25 - 50$ GHz overmoded spectral region. We note that the shielding (ratio of maximum interior field component to incident field) in this example, provided by the canonical enclosure, is not very significant (-5.9 to -8.5 dB). The interior field is then used to drive interior cables and the induced voltages are estimated. The delivered power to an antenna with matched load is also estimated. The resulting estimated drive levels already contain margins because of the use of bounding estimates for power reception and for cable coupling and resonant voltage transformations along cables.

Screening levels for voltage upset and no-fire power for ordnance are reviewed and compared to these bounding coupling levels. Although in our example there is considerable margin for the power coupling, the induced voltages for the unshielded cable (using the limited enclosure shielding) are somewhat above conservative digital logic voltage threshold screening levels. Nevertheless, shielded cables would be expected to reduce these induced voltage levels to near or below the screening values.

This page left blank

7 APPENDIX I: INTERIOR DRIVE FIELDS

The drive field of the cables on the interior of a typical barrier is first estimated using canonical sets of parameters as an illustration.

7.1 Interior Field Environment*

Using conservation of steady state power in a linear system the received power through a port of entry (POE) can be equated to the interior power lost [20], [16], which includes power lost to the conducting walls as well as dielectric losses, etc.

$$P_{rec} = P_{wall} + \cdots \tag{240}$$

At very high frequencies we can approximate this as the power transmitted through the port of entry, taken as a narrow slot aperture, into an empty half space, but include power lost (which consists of power absorbed and transmitted back out) on the right hand side

$$P_{trans} = \langle P_{loss} \rangle + P_{wall} + \cdots = \langle P_{trans} \rangle + \langle P_{abs} \rangle + P_{wall} + \cdots \tag{241}$$

However, at very high frequencies we can approximate the right hand side neglecting the aperture loss terms to overestimate the power lost on the interior

$$P_{trans} \approx P_{wall} + \cdots \tag{242}$$

In addition, because in a linear steady state operation average power is conserved, we can also make use of these received or transmitted power estimates at various levels of the system topology to compare directly with power thresholds of interior electroexplosive components.

7.1.1 Slot Aperture Penetration

The electromagnetic transmission through a narrow slot aperture, in general including electrically large depth is taken as the input. We assume that the cavity is highly overmoded and we can use transmission into an empty half space as an approximation (also because the slot will be electrically long distributed load matching would be highly improbable). We can write the Deep slot transmission as

$$P_{trans}^{Deep} = \sigma_{trans}^{Deep} S_{inc} \tag{243}$$

with cross section [17], [18]

$$\sigma_{trans}^{Deep} \approx \frac{\lambda \ell}{\pi} p_{slot} q_{trans}^{Deep} \tag{244}$$

and incident field $\underline{H}^{inc} = H_0 \underline{e}_{inc}$ polarization mismatch factor (with z-directed slot length)

$$p_{slot} = \left(\underline{e}_\theta \cdot \underline{H}^{inc}\right)^2 / \left|\underline{H}^{inc}\right|^2 = \left(\underline{e}_\theta \cdot \underline{e}_{inc}\right)^2 \tag{245}$$

as well as wall loss mismatch factor at the slot resonances (where the reactive terms vanish) [18]

$$q_{trans}^{Deep} = \frac{G_{rad}^2}{\left[R_{int}^{intr} / \left(2 Z_0^{intr2}\right) + G_{rad}\right]^2} \tag{246}$$

with incident Poynting vector magnitude

$$S_{inc} = \eta_0 \left|H_0\right|^2 \tag{247}$$

slot interior characteristic impedance

$$Z_0^{intr} = \eta_0 w/d \tag{248}$$

and wall loss

$$R_{int}^{intr} = 2R_s/d \tag{249}$$

and radiation conductance fit [18]

$$\pi h \eta_0 G_{rad} \approx \pi kh \left[1 - \left(\frac{\pi}{2kh}\right)^2 + \frac{1}{2}\left(\frac{\pi}{2kh}\right)^4\right], kh \geq \pi/2 \tag{250}$$

7.1.2 Wall Cross Section And Quality Factor

The wall loss power and cross section can be written as [16]

$$P_{wall} = \sigma_{wall} S \tag{251}$$

where

$$\sigma_{wall} = \frac{4}{3} A R_s/\eta_0 \tag{252}$$

and

$$S = \eta_0 \left\langle \left|\underline{H}\right|^2 \right\rangle = 3\eta_0 \left\langle \left|H_i\right|^2 \right\rangle \tag{253}$$

7.1.3 Average & Extreme Interior Field Environment

The interior field level is estimated for a canonical shield and cavity.

$$\sigma_{rec} S_{inc} = \sigma_{wall} S + \cdots \tag{254}$$

$$\sigma_{trans} S_{inc} = \langle \sigma_{loss} \rangle S + \sigma_{wall} S + \cdots = \langle \sigma_{trans} \rangle S + \langle \sigma_{abs} \rangle S + \sigma_{wall} S + \cdots \tag{255}$$

One Complex Component Now for equal statistics on real and imaginary parts of the field [23]

$$u_{jr} = E_{jr}/E_0 \tag{256}$$

$$u_{ji} = E_{ji}/E_0 \tag{257}$$

where the magnitude is

$$E_0 = \sqrt{\left|E\right|^2} = \sqrt{E_{jr}^2 + E_{ji}^2} \tag{258}$$

and thus

$$u_0 = 1/\sqrt{2} \tag{259}$$

Then the square of the magnitude is

$$w_j = p_{jr}^2 + p_{ji}^2 \tag{260}$$

with density

$$p_{w_j}(w_j) = e^{-w_j} \tag{261}$$

mean value

$$\langle w_j \rangle = \int_0^\infty w_j p_{w_j}(w_j)\, dw_j = \left[-w_j e^{-w_j} - e^{-w_j}\right]_0^\infty = 1 \tag{262}$$

and distribution function

$$F_{w_j}(w_j) = \int_0^{w_j} p_{w_j}(w_j)\, dw_j = 1 - e^{-w_j} \tag{263}$$

where values are

$$F_{w_j}(3) \approx 0.95 \tag{264}$$

$$F_{w_j}(9/2) = 0.98889 \approx 0.99 \tag{265}$$

$$F_{w_j}(9) = 0.99987 \approx 0.9999 \tag{266}$$

$$\langle w_j \rangle = 1 \tag{267}$$

If we have an electric field component in the overmoded region which has normally distributed real and imaginary parts then the normalized square of the magnitude of this component $XM = |E_x|^2$, where M is the mean of the distribution, has density

$$f_X(x) = e^{-x}\ ,\ 0 < x < \infty \tag{268}$$

where

$$\int_0^\infty f_X(x)\, dx = \int_0^\infty e^{-x} dx = 1 \tag{269}$$

with unit mean

$$\langle x \rangle = \int_0^\infty x f_X(x)\, dx = \int_0^\infty x e^{-x} dx = -\left(x e^{-x} + e^{-x}\right)_0^\infty = 1 \tag{270}$$

and distribution

$$F_X(x) = \int_0^x f_X(x)\, dx = 1 - e^{-x} \tag{271}$$

If we take a 95% confidence level as an extreme we find a peak to average ratio $x \approx 3$. If we take a 99% confidence as an extreme we find a peak to average ratio $x \approx 9/2$. This second level corresponds to a field peak to average ratio of $3/\sqrt{2} \approx 2.1$.

7.1.4 Average & Extreme Interior Field Environment*

An example we take a slot length $\ell = 2h \approx 2$ in, slot depth $d \approx 0.5$ in, slot width $w = 0.002$ in, aluminum slot and cavity walls $\mu = \mu_0$, $\sigma \approx 2.6 \times 10^7$ S/m, and cavity area $A \approx 0.5$ m^2. Evaluation at $f = 25 - 50$ GHz gives (using the preceding Deep slot formulas) gives

$$\sigma_{trans}^{Deep} \approx \frac{\lambda \ell}{\pi} p_{slot} q_{trans}^{Deep} \leq 3.0148 - 2.2277 \times 10^{-5} \text{ m}^2 \tag{272}$$

$$q_{trans}^{Deep} = \frac{G_{rad}^2}{\left[R_{int}^{intr} / \left(2Z_0^{intr2}\right) + G_{rad}\right]^2} \approx 0.15548 - 0.22977 \tag{273}$$

$$S_{inc} = \eta_0 \left|H_0^{inc}\right|^2 = \left|E_0^{inc}\right|^2 / \eta_0 \tag{274}$$

$$S = \eta_0 \left\langle \left|\underline{H}\right|^2 \right\rangle = 3\eta_0 \left\langle |H_i|^2 \right\rangle = \left\langle \left|\underline{E}\right|^2 \right\rangle / \eta_0 = 3 \left\langle |E_i|^2 \right\rangle / \eta_0 \tag{275}$$

$$Z_0^{intr} = \eta_0 w/d \approx 1.5069 \text{ ohms} \tag{276}$$

$$R_{int}^{intr} = 2R_s/d \approx 9.7026 - 13.722 \text{ ohms/m} \tag{277}$$

$$G_{rad} \sim k/\eta_0 \approx 1.3908 - 2.7816 \text{ S/m} \tag{278}$$

$$\left\langle \sigma_{trans}^{Deep} \right\rangle = q_{trans}^{Deep} 2 \frac{\lambda^2}{4\pi} \frac{1}{2} \approx 1.7792 - 0.65732 \times 10^{-6} \text{ m}^2 \tag{279}$$

$$\left\langle \sigma_{abs}^{Deep} \right\rangle = q_{abs}^{Deep} 2 \frac{\lambda^2}{4\pi} \frac{1}{2} \approx 5.466 - 1.428 \times 10^{-6} \text{ m}^2 \tag{280}$$

$$q_{abs}^{Deep} \approx \frac{2G_{rad} R_{int}^{intr} / \left(2Z_0^{intr2}\right)}{\left[G_{rad} + R_{int}^{intr} / \left(2Z_0^{intr2}\right)\right]^2} \approx 0.47766 - 0.49915 \tag{281}$$

$$\sigma_{wall} = \frac{4}{3} A R_s / \eta_0 \approx 1.0903 - 1.5419 \times 10^{-4} \text{ m}^2 \tag{282}$$

These result in the average shielding effectiveness

$$S/S_{inc} \approx \frac{\sigma_{trans}^{Deep}}{\left\langle \sigma_{trans}^{Deep} \right\rangle + \left\langle \sigma_{abs}^{Deep} \right\rangle + \sigma_{wall}}$$

$$\approx \frac{0.30148}{1.0903 + 0.05466 + 0.017792} - \frac{0.22277}{1.5419 + 0.01428 + 0.0065732} \approx 0.2593 - 0.1425 \tag{283}$$

with

$$\left\langle |H_i|^2 \right\rangle / \left|H_0^{inc}\right|^2 \approx 0.0864 - 0.0475 \, (-10.6 \text{ to } -13.2 \text{ dB}) \approx \left\langle |E_i|^2 \right\rangle / \left|E_0^{inc}\right|^2 \tag{284}$$

and using the overmoded distribution

$$\left|E_i\right|^2 / \left|E_0^{inc}\right|^2 \leq 3 \left\langle \left|E_i\right|^2 \right\rangle / \left|E_0^{inc}\right|^2 \approx 0.2593 - 0.1425 \left(-5.9 \text{ to } -8.5 \text{ dB}\right) \text{ , 95\% confidence} \tag{285}$$

$$\left|E_i\right|^2 / \left|E_0^{inc}\right|^2 \leq \frac{9}{2} \left\langle \left|E_i\right|^2 \right\rangle / \left|E_0^{inc}\right|^2 \approx 0.389 - 0.214 \text{ , 99\% confidence} \tag{286}$$

If we take as an example $V \approx 0.01$ m^3 we find the quality factor from cavity wall losses

$$Q_{wall} = \frac{\omega \mu_0 \left\langle \left|\underline{H}\right|^2 \right\rangle_V V}{R_s \left\langle \left|\underline{H}\right|^2 \right\rangle_S A} \sim \frac{3k\eta_0 V}{4R_s A} = \frac{3V}{2\delta A} \approx 48,000 - 68,000 \text{ , if } \mu = \mu_0 \tag{287}$$

and the average with slot losses

$$\langle Q \rangle = \frac{kSV}{S \left\langle \sigma_{trans}^{Deep} \right\rangle + S \left\langle \sigma_{abs}^{Deep} \right\rangle + S\sigma_{wall}} = \frac{kV}{\left\langle \sigma_{trans}^{Deep} \right\rangle + \left\langle \sigma_{abs}^{Deep} \right\rangle + \sigma_{wall}} \approx 45,000 - 67,000 \tag{288}$$

These result in the modal overlap parameter which is reasonably large compared to unity

$$\alpha = \frac{k^3 V}{2\pi Q} \approx \frac{k^3 \delta A}{3\pi} \approx 5 - 27 \tag{289}$$

This page left blank

8 APPENDIX II - SHIELDED CABLE COUPLING & PENETRATION

We now estimate coupling to pins within a shielded canonical cable [24], [25] again with the electric field in the plane of the cable transmission line (cable and neighboring return chassis) axis. The transmission line equations for the shield (neglecting the transfer terms to the cable interior assuming the cable shield is effective in reducing the interior cable current [26]) are

$$\frac{dV_s}{dz} + Z_s I_s = -i\omega L_s^i H_0 = -ik2h_e^s \eta_0 H_0 e^{ikz\cos\theta_0} \tag{290}$$

$$\frac{dI_s}{dz} + Y_s V_s = i\omega C_s^i E_0 \cos\theta_0 = ik2h_e^s \frac{E_0\cos\theta_0}{\sqrt{L_s/C_s}} e^{ikz\cos\theta_0} \tag{291}$$

Eliminating the voltage gives

$$\begin{aligned}\left(\frac{d^2}{dz^2} + \Gamma_s^2\right) I_s &= 2h_e^s \left(-k^2 \frac{E_0\cos\theta_0}{\sqrt{L_s/C_s}} \cos\theta_0 + Y_s ik\eta_0 H_0\right) e^{ikz\cos\theta_0} \\ &= 2h_e^s \left(-\omega C_s k^2 \frac{E_0}{\omega\sqrt{L_s C_s}} \cos^2\theta_0 + \omega C_s k\eta_0 H_0\right) e^{ikz\cos\theta_0} \\ &= k2h_e^s \omega C_s \left(-E_0\cos^2\theta_0 + \eta_0 H_0\right) e^{ikz\cos\theta_0}\end{aligned} \tag{292}$$

or

$$\left(\frac{d^2}{dz^2} + \Gamma_s^2\right) I_s = k2h_e^s \omega C_s E_0 \sin^2\theta_0 e^{ikz\cos\theta_0} \tag{293}$$

where

$$\Gamma_s^2 = -Z_s Y_s \tag{294}$$

$$E_0 = \eta_0 H_0 \tag{295}$$

$$k = \omega\sqrt{L_s C_s} \tag{296}$$

$$L_s^i/\mu_0 = 2h_e^s = C_s^i/C_s \tag{297}$$

The shield current is then

$$\begin{aligned}I_s(z) &= c_{0s}\cos(\Gamma_s z) + c_{1s}\sin(\Gamma_s z) + k2h_e^s \omega C_s \left(-E_0\cos^2\theta_0 + \eta_0 H_0\right) e^{ikz\cos\theta_0} / \left(\Gamma_s^2 - k^2\cos^2\theta_0\right) \\ &= c_{0s}\cos(\Gamma_s z) + c_{1s}\sin(\Gamma_s z) + k2h_e^s \omega C_s E_0 \sin^2\theta_0 e^{ikz\cos\theta_0} / \left(\Gamma_s^2 - k^2\cos^2\theta_0\right)\end{aligned} \tag{298}$$

8.0.5 Shield With Shorted Ends

In many cases the shield is terminated in conductors attached to chassis at the ends so it seems reasonable to apply boundary conditions on the shield terminated at both ends

$$V_s(0) = 0 = V_s(\ell) \tag{299}$$

The boundary condition $V_s(0) = 0$ using the preceding current transmission line equation gives

$$\frac{dI_s}{dz}(0) = ik2h_e^s \frac{E_0 \cos\theta_0}{\sqrt{L_s/C_s}} \tag{300}$$

which means

$$c_{1s}\Gamma_s + k2h_e^s \omega C_s E_0 ik \cos\theta_0 \sin^2\theta_0 / \left(\Gamma_s^2 - k^2\cos^2\theta_0\right) = ik2h_e^s \frac{E_0\cos\theta_0}{\sqrt{L_s/C_s}} \tag{301}$$

or

$$c_{1s}\Gamma_s = i2h_e^s E_0 \omega C_s \cos\theta_0 \frac{\Gamma_s^2 - k^2}{\Gamma_s^2 - k^2\cos^2\theta_0} \tag{302}$$

The boundary condition $0 = V_s(\ell)$ also gives

$$\frac{dI_s}{dz}(\ell) = ik2h_e^s \frac{E_0\cos\theta_0}{\sqrt{L_s/C_s}} e^{ik\ell\cos\theta_0} = i2h_e^s \omega C_s E_0 \cos\theta_0 e^{ik\ell\cos\theta_0} \tag{303}$$

where

$$\frac{dI_s}{dz} = -c_{0s}\Gamma_s \sin(\Gamma_s z) + c_{1s}\Gamma_s \cos(\Gamma_s z) + ik^2 2h_e^s \omega C_s \eta_0 H_0 \sin^2\theta_0 \cos\theta_0 e^{ikz\cos\theta_0} / \left(\Gamma_s^2 - k^2\cos^2\theta_0\right)$$

$$= -c_{0s}\Gamma_s \sin(\Gamma_s z) + i2h_e^s E_0 \omega C_s \cos\theta_0 \frac{1}{\Gamma_s^2 - k^2\cos^2\theta_0}\left[\left(\Gamma_s^2 - k^2\right)\cos(\Gamma_s z) + k^2\sin^2\theta_0 e^{ikz\cos\theta_0}\right] \tag{304}$$

or

$$c_{0s}\Gamma_s \sin(\Gamma_s \ell) = i2h_e^s E_0 \omega C_s \cos\theta_0 \frac{\Gamma_s^2 - k^2}{\Gamma_s^2 - k^2\cos^2\theta_0}\left[\cos(\Gamma_s\ell) - e^{ik\ell\cos\theta_0}\right] \tag{305}$$

so we can write

$$\frac{dI_s}{dz} = -i2h_e^s E_0 \omega C_s \cos\theta_0 \frac{\Gamma_s^2 - k^2}{\Gamma_s^2 - k^2\cos^2\theta_0}\left[\cos(\Gamma_s\ell) - e^{ik\ell\cos\theta_0}\right]\frac{\sin(\Gamma_s z)}{\sin(\Gamma_s\ell)}$$

$$+i2h_e^s E_0 \omega C_s \cos\theta_0 \frac{1}{\Gamma_s^2 - k^2\cos^2\theta_0}\left[\left(\Gamma_s^2 - k^2\right)\cos(\Gamma_s z) + k^2\sin^2\theta_0 e^{ikz\cos\theta_0}\right] \tag{306}$$

The c_{0s} (first) term exhibits a resonant enhancement when

$$\Gamma_s'\ell = m\pi \tag{307}$$

with functional behavior

$$V_s(z) \sim c_{1s} \sin(\Gamma'_s z) \tag{308}$$

However, we note for $\Gamma_s \to k$

$$\frac{dI_s}{dz} = i2h_e^s \omega C_s E_0 \cos\theta_0 e^{ikz\cos\theta_0} \tag{309}$$

8.0.6 Shield With Loaded End

Suppose there is an extra inductance at one end of the shield so that we can approximately apply

$$V_s(0) = 0 \approx I_s(\ell) \tag{310}$$

Eliminating the voltage again gives the shield current

$$I_s(z) = c_{0s}\cos(\Gamma_s z) + c_{1s}\sin(\Gamma_s z) + k2h_e^s \omega C_s E_0 \sin^2\theta_0 e^{ikz\cos\theta_0} / \left(\Gamma_s^2 - k^2\cos^2\theta_0\right) \tag{311}$$

The boundary condition $V_s(0) = 0$ using the preceding current transmission line equation gives

$$\frac{dI_s}{dz}(0) = i2h_e^s \omega C_s E_0 \cos\theta_0 \tag{312}$$

which means

$$c_{1s}\Gamma_s + i2h_e^s \omega C_s E_0 \cos\theta_0 k^2 \sin^2\theta_0 / \left(\Gamma_s^2 - k^2\cos^2\theta_0\right) = i2h_e^s \omega C_s E_0 \cos\theta_0 \tag{313}$$

or

$$c_{1s}\Gamma_s = i2h_e^s E_0 \omega C_s \cos\theta_0 \frac{\Gamma_s^2 - k^2}{\Gamma_s^2 - k^2\cos^2\theta_0} \tag{314}$$

The boundary condition $0 = I_s(\ell)$ also gives

$$c_{0s}\cos(\Gamma_s \ell) = -i2h_e^s E_0 \omega C_s \frac{\cos\theta_0 \left(\Gamma_s^2 - k^2\right)\sin(\Gamma_s \ell)/\Gamma_s - ik\sin^2\theta_0 e^{ik\ell\cos\theta_0}}{\Gamma_s^2 - k^2\cos^2\theta_0} \tag{315}$$

Then

$$\frac{dI_s}{dz}(z) = -c_{0s}\Gamma_s \sin(\Gamma_s z) + c_{1s}\Gamma_s \cos(\Gamma_s z) + ik^2 2h_e^s \omega C_s E_0 \cos\theta_0 \sin^2\theta_0 e^{ikz\cos\theta_0} / \left(\Gamma_s^2 - k^2\cos^2\theta_0\right) \tag{316}$$

or

$$\frac{dI_s}{dz}(z) = i2h_e^s E_0 \omega C_s \frac{\cos\theta_0 \left(\Gamma_s^2 - k^2\right)\sin(\Gamma_s \ell)/\Gamma_s - ik\sin^2\theta_0 e^{ik\ell\cos\theta_0}}{\Gamma_s^2 - k^2\cos^2\theta_0} \frac{\Gamma_s \sin(\Gamma_s z)}{\cos(\Gamma_s \ell)}$$

$$+i2h_e^s E_0 \omega C_s \cos\theta_0 \frac{\Gamma_s^2 - k^2}{\Gamma_s^2 - k^2\cos^2\theta_0}\cos(\Gamma_s z) + ik^2 2h_e^s \omega C_s E_0 \cos\theta_0 \sin^2\theta_0 e^{ikz\cos\theta_0} / \left(\Gamma_s^2 - k^2\cos^2\theta_0\right) \tag{317}$$

If we are near the resonance $\Gamma'_s \ell = (n - 1/2)\pi$

$$\frac{dI_s}{dz}(z) \sim i2h_e^s E_0 \omega C_s \frac{\cos\theta_0 \left(\Gamma_s^2 - k^2\right)\sin(\Gamma_s \ell)/\Gamma_s - ik\sin^2\theta_0 e^{ik\ell\cos\theta_0}}{\Gamma_s^2 - k^2\cos^2\theta_0} \frac{\Gamma_s \sin(\Gamma_s z)}{\cos(\Gamma_s \ell)} \tag{318}$$

We note that if $\Gamma_s' \to k$ we can write this as

$$\frac{dI_s}{dz}(z) \sim 2h_e^s E_0 \frac{\omega C_s}{k} e^{ik\ell\cos\theta_0} \frac{\Gamma_s \sin(\Gamma_s z)}{\cos(\Gamma_s \ell)} \tag{319}$$

8.1 Coaxial Region

The interior coaxial equations

$$\frac{dV_c}{dz} + Z_c I_c = Z_T I_s \tag{320}$$

$$\frac{dI_c}{dz} + Y_c V_c = -Y_T V_s = i\omega (C_T/C_s) q_{sh} = (C_T/C_s) \frac{dI_s}{dz} \tag{321}$$

give

$$\left(\frac{d^2}{dz^2} + \Gamma_c^2\right) V_c = (Z_T - Z_c C_T/C_s) \frac{dI_s}{dz} \tag{322}$$

where

$$\Gamma_c^2 = -Z_c Y_c \tag{323}$$

where we can again take boundary conditions as

$$V_c(0) = 0 = I_c(\ell) \tag{324}$$

The transfer immittances Z_T and Y_T (and C_T) for standard cables can be estimated by using the semi-empirical results [27].

8.1.1 Drive With Shorted Ends

The drive with both ends shorted gives

$$V_c(z) = c_{0c}\cos(\Gamma_c z) + c_{1c}\sin(\Gamma_c z)$$

$$-i2h_e^s E_0 \omega C_s \cos\theta_0 \frac{\left(\Gamma_s^2 - k^2\right)/\left(\Gamma_c^2 - \Gamma_s^2\right)}{\Gamma_s^2 - k^2\cos^2\theta_0} \left[\cos(\Gamma_s \ell) - e^{ik\ell\cos\theta_0}\right] \frac{\sin(\Gamma_s z)}{\sin(\Gamma_s \ell)} (Z_T - Z_c C_T/C_s)$$

$$+i2h_e^s E_0 \omega C_s \cos\theta_0 \frac{1}{\Gamma_s^2 - k^2\cos^2\theta_0} \left[\left(\frac{\Gamma_s^2 - k^2}{\Gamma_c^2 - \Gamma_s^2}\right)\cos(\Gamma_s z) + \frac{k^2\sin^2\theta_0}{\Gamma_c^2 - k^2\cos^2\theta_0} e^{ikz\cos\theta_0}\right] (Z_T - Z_c C_T/C_s) \tag{325}$$

The left boundary condition $V_c(0) = 0$ gives

$$c_{0c} = -i2h_e^s E_0 \omega C_s \cos\theta_0 \frac{1}{\Gamma_s^2 - k^2\cos^2\theta_0} \left[\left(\frac{\Gamma_s^2 - k^2}{\Gamma_c^2 - \Gamma_s^2}\right) + \frac{k^2\sin^2\theta_0}{\Gamma_c^2 - k^2\cos^2\theta_0}\right] (Z_T - Z_c C_T/C_s) \tag{326}$$

and the right boundary condition $0 = I_c(\ell)$ gives

$$\frac{dV_c}{dz}(\ell) + Z_c I_c(\ell) = Z_T I_s(\ell) \rightarrow \frac{dV_c}{dz}(\ell) = Z_T I_s(\ell) \tag{327}$$

where

$$I_s(\ell) = i2h_e^s E_0 \omega C_s \cos\theta_0 \frac{\left(\Gamma_s^2 - k^2\right)/\Gamma_s}{\Gamma_s^2 - k^2\cos^2\theta_0}\left[1 - e^{ik\ell\cos\theta_0}\cos(\Gamma_s\ell)\right]\frac{1}{\sin(\Gamma_s\ell)}$$

$$+k2h_e^s\omega C_s E_0 \sin^2\theta_0 \frac{e^{ik\ell\cos\theta_0}}{\Gamma_s^2 - k^2\cos^2\theta_0} \tag{328}$$

8.1.2 Drive With Open-Short Ends

$$V_c(z) = c_{0c}\cos(\Gamma_c z) + c_{1c}\sin(\Gamma_c z)$$

$$+i2h_e^s E_0\omega C_s \frac{\cos\theta_0\left(\Gamma_s^2 - k^2\right)\sin(\Gamma_s\ell)/\Gamma_s - ik\sin^2\theta_0 e^{ik\ell\cos\theta_0}}{\left(\Gamma_s^2 - k^2\cos^2\theta_0\right)\left(\Gamma_c^2 - \Gamma_s^2\right)}\frac{\Gamma_s\sin(\Gamma_s z)}{\cos(\Gamma_s\ell)}\left(Z_T - Z_c C_T/C_s\right)$$

$$+i2h_e^s E_0\omega C_s\cos\theta_0\frac{\left(\Gamma_s^2 - k^2\right)/\left(\Gamma_c^2 - \Gamma_s^2\right)}{\left(\Gamma_s^2 - k^2\cos^2\theta_0\right)}\cos(\Gamma_s z)\left(Z_T - Z_c C_T/C_s\right)$$

$$+i2h_e^s\omega C_s E_0\cos\theta_0\frac{k^2\sin^2\theta_0}{\left(\Gamma_s^2 - k^2\cos^2\theta_0\right)\left(\Gamma_c^2 - \Gamma_s^2\right)}e^{ikz\cos\theta_0}\left(Z_T - Z_c C_T/C_s\right) \tag{329}$$

The left boundary condition $V_c(0) = 0$ gives

$$c_{0c} = -i2h_e^s E_0\omega C_s\cos\theta_0\frac{1}{\left(\Gamma_c^2 - \Gamma_s^2\right)}\left(Z_T - Z_c C_T/C_s\right) \tag{330}$$

The boundary condition $0 = I_c(\ell)$ then gives

$$\frac{dV_c}{dz}(\ell) + Z_c I_c(\ell) = Z_T I_s(\ell) \rightarrow \frac{dV_c}{dz}(\ell) = 0 \tag{331}$$

This page left blank

8.2 APPENDIX III: ANTENNA DRIVING NONUNIFORM TRANSMISSION LINE

Suppose we examine the case of a nonuniform transmission line

$$\frac{dV}{dz} = -Z(z)\, I \tag{332}$$

$$\frac{dI}{dz} = -Y(z)\, V \tag{333}$$

$$\frac{d^2 I}{dz^2} = (Y'/Y)\frac{dI}{dz} + YZI \tag{334}$$

For simplicity we take

$$Y = Y_l \ell / z \tag{335}$$

$$Z = Z_l z / \ell \tag{336}$$

gives

$$\frac{d^2 I}{dz^2} + \frac{1}{z}\frac{dI}{dz} - Y_l Z_l I = 0 \tag{337}$$

The general solution is

$$I = c_0 J_0(\Gamma_l z) + c_1 Y_0(\Gamma_l z) \tag{338}$$

where

$$\Gamma_l^2 = -Z_l Y_l \tag{339}$$

Let us impose

$$V(\ell_1) = -\frac{1}{Y(\ell_1)}\frac{dI}{dz}(\ell_1) = V_{oc} - I(\ell_1) Z_s \tag{340}$$

or

$$V_{oc} - [c_0 J_0(\Gamma_l \ell_1) + c_1 Y_0(\Gamma_l \ell_1)] Z_s = [c_0 J_1(\Gamma_l \ell_1) + c_1 Y_1(\Gamma_l \ell_1)](\ell_1/\ell)\Gamma_l / Y_l \tag{341}$$

$$\Gamma_l / Y_l = -Z_l \Gamma_l / (-Z_l Y_l) = -Z_l / \Gamma_l = i Z_{l0} \tag{342}$$

$$Z_{l0} = \sqrt{Z_l / Y_l} \tag{343}$$

and

$$I(\ell) = 0 \rightarrow c_0 J_0(\Gamma_l \ell) = -c_1 Y_0(\Gamma_l \ell) \tag{344}$$

Then

$$V_{oc} - c_0 \left[J_0(\Gamma_l \ell_1) - \frac{J_0(\Gamma_l \ell)}{Y_0(\Gamma_l \ell)} Y_0(\Gamma_l \ell_1) \right] Z_s = c_0 \left[J_1(\Gamma_l \ell_1) - \frac{J_0(\Gamma_l \ell)}{Y_0(\Gamma_l \ell)} Y_1(\Gamma_l \ell_1) \right] (\ell_1/\ell)\Gamma_l / Y_l$$

$$V_{oc} = c_0 \left[\left\{ J_0 \left(\Gamma_l \ell_1 \right) - \frac{J_0 \left(\Gamma_l \ell \right)}{Y_0 \left(\Gamma_l \ell \right)} Y_0 \left(\Gamma_l \ell_1 \right) \right\} Z_s + \left\{ J_1 \left(\Gamma_l \ell_1 \right) - \frac{J_0 \left(\Gamma_l \ell \right)}{Y_0 \left(\Gamma_l \ell \right)} Y_1 \left(\Gamma_l \ell_1 \right) \right\} \left(\ell_1 / \ell \right) i Z_{l0} \right] \tag{345}$$

The voltage at the open circuit end is

$$V \left(\ell \right) = -\frac{1}{Y \left(\ell \right)} \frac{dI}{dz} \left(\ell \right) = \frac{\Gamma_l}{Y_l} c_0 \left[J_1 \left(\Gamma_l \ell \right) - \frac{J_0 \left(\Gamma_l \ell \right)}{Y_0 \left(\Gamma_l \ell \right)} Y_1 \left(\Gamma_l \ell \right) \right] = \frac{\Gamma_l}{Y_l} \frac{c_0}{Y_0 \left(\Gamma_l \ell \right)} \left[J_1 \left(\Gamma_l \ell \right) Y_0 \left(\Gamma_l \ell \right) - J_0 \left(\Gamma_l \ell \right) Y_1 \left(\Gamma_l \ell \right) \right]$$

$$= \frac{2}{\pi Y_l \ell} \frac{c_0}{Y_0 \left(\Gamma_l \ell \right)} \tag{346}$$

Note also

$$V \left(\ell_1 \right) = -\frac{1}{Y \left(\ell_1 \right)} \frac{dI}{dz} \left(\ell_1 \right) = c_0 \left[J_1 \left(\Gamma_l \ell_1 \right) - \frac{J_0 \left(\Gamma_l \ell \right)}{Y_0 \left(\Gamma_l \ell \right)} Y_1 \left(\Gamma_l \ell_1 \right) \right] \left(\ell_1 / \ell \right) \Gamma_l / Y_l \tag{347}$$

so that

$$V \left(\ell \right) / V \left(\ell_1 \right) = \frac{2/\pi}{\Gamma_l \ell_1 \left[J_1 \left(\Gamma_l \ell_1 \right) Y_0 \left(\Gamma_l \ell \right) - J_0 \left(\Gamma_l \ell \right) Y_1 \left(\Gamma_l \ell_1 \right) \right]} \tag{348}$$

Thus

$$\frac{V \left(\ell \right)}{V_{oc}} = \frac{2 / \left(\pi Y_l \ell \right)}{\left\{ J_0 \left(\Gamma_l \ell_1 \right) Y_0 \left(\Gamma_l \ell \right) - J_0 \left(\Gamma_l \ell \right) Y_0 \left(\Gamma_l \ell_1 \right) \right\} Z_s + \left\{ J_1 \left(\Gamma_l \ell_1 \right) Y_0 \left(\Gamma_l \ell \right) - J_0 \left(\Gamma_l \ell \right) Y_1 \left(\Gamma_l \ell_1 \right) \right\} \left(\ell_1 / \ell \right) i Z_{l0}} \tag{349}$$

If we take $\Gamma_l \ell_1 \to 0$

$$\frac{V \left(\ell \right)}{V_{oc}} \sim \frac{2 / \left(\pi Y_l \ell \right)}{\left\{ Z_s + \left(\Gamma_l \ell_1 / 2 \right) \left(\ell_1 / \ell \right) i Z_{l0} \right\} Y_0 \left(\Gamma_l \ell \right) + \left\{ i Z_{l0} 2 / \left(\pi \Gamma_l \ell \right) - \left(2/\pi \right) \ln \left(\Gamma_l \ell e^{\gamma} / 2 \right) Z_s \right\} J_0 \left(\Gamma_l \ell \right)} \tag{350}$$

and

$$V \left(\ell \right) / V \left(\ell_1 \right) \sim \frac{1}{J_0 \left(\Gamma_l \ell \right) + \left(\Gamma_l \ell_1 / 2 \right)^2 \pi Y_0 \left(\Gamma_l \ell \right)} \tag{351}$$

If we set

$$Z_s Y_0 \left(\Gamma_l \ell \right) - \left(2/\pi \right) \ln \left(\Gamma_l \ell e^{\gamma} / 2 \right) Z_s J_0 \left(\Gamma_l \ell \right) = 0 \tag{352}$$

then

$$\frac{V \left(\ell \right)}{V_{oc}} \sim \frac{1}{\left(\Gamma_l \ell_1 \right)^2 \left(\pi / 4 \right) Y_0 \left(\Gamma_l \ell \right) + J_0 \left(\Gamma_l \ell \right)} \tag{353}$$

If we take

$$J_0 \left(\Gamma_l \ell \right) = J_0 \left(j_{0p} \right) = 0 \tag{354}$$

$$\frac{V(\ell)}{V_{oc}} \sim \frac{1}{(j_{0p}\ell_1/\ell)^2(\pi/4)Y_0(j_{0p})} = \frac{1}{(\Gamma_l\ell_1/2)^2\pi Y_0(j_{0p})} >> 1 \tag{355}$$

$$V(\ell)/V(\ell_1) \sim \frac{1}{(\Gamma_l\ell_1/2)^2\pi Y_0(j_{0p})} >> 1 \tag{356}$$

$$Y_0(j_{0p}) \sim \sqrt{\frac{2}{\pi j_{0p}}}\sin(j_{0p}-\pi/4) \sim \sqrt{\frac{2}{\pi j_{0p}}}\sin(p\pi-\pi/2) = \sqrt{\frac{2}{\pi j_{0p}}}(-1)^{p-1} \tag{357}$$

$$j_{0p} \sim (p-1/4)\pi \tag{358}$$

$$\frac{V(\ell)}{V_{oc}} \sim \frac{\sqrt{\Gamma_l\ell/2}(-1)^{p-1}}{(\Gamma_l\ell_1/2)^2\pi^{1/2}} >> 1 \tag{359}$$

$$V(\ell)/V(\ell_1) \sim \frac{\sqrt{\Gamma_l\ell/2}(-1)^{p-1}}{(\Gamma_l\ell_1/2)^2\pi^{1/2}} >> 1 \tag{360}$$

from which we infer that

$$V(\ell_1) \sim V_{oc} \tag{361}$$

or that $Z_i >> Z_s$.

What if we arrange the right termination to be "matched" in the sense that

$$I(z) = c_0 H_0^{(1)}(\Gamma_l z) \tag{362}$$

The voltage at the left termination is

$$V(\ell_1) = -\frac{1}{Y(\ell_1)}\frac{dI}{dz}(\ell_1) = \frac{\Gamma_l}{Y(\ell_1)}c_0 H_1^{(1)}(\Gamma_l\ell_1) \tag{363}$$

The voltage at the right termination is

$$V(\ell) = -\frac{1}{Y(\ell)}\frac{dI}{dz}(\ell) = \frac{\Gamma_l}{Y(\ell)}c_0 H_1^{(1)}(\Gamma_l\ell) \tag{364}$$

The ratio is

$$V(\ell)/V(\ell_1) = \frac{Y(\ell_1)}{Y(\ell)}\frac{H_1^{(1)}(\Gamma_l\ell)}{H_1^{(1)}(\Gamma_l\ell_1)} = (\ell/\ell_1)\frac{H_1^{(1)}(\Gamma_l\ell)}{H_1^{(1)}(\Gamma_l\ell_1)} \tag{365}$$

Then if we take $\Gamma_l\ell_1 << 1$

$$V(\ell)/V(\ell_1) \sim i\frac{\pi}{2}\Gamma_l\ell H_1^{(1)}(\Gamma_l\ell) \tag{366}$$

or

$$V(\ell)/V(\ell_1) \sim \sqrt{\pi\Gamma_l\ell/2}e^{i(\Gamma_l\ell-\pi/4)} \tag{367}$$

or

$$|V(\ell)/V(\ell_1)| \sim \sqrt{\pi\Gamma_l\ell/2} >> 1 \tag{368}$$

Also

$$Z_i = V(\ell_1)/I(\ell_1) = \frac{\Gamma_l}{Y(\ell_1)}\frac{H_1^{(1)}(\Gamma_l\ell_1)}{H_0^{(1)}(\Gamma_l\ell_1)} = \frac{\Gamma_l\ell_1}{Y_l\ell}\frac{H_1^{(1)}(\Gamma_l\ell_1)}{H_0^{(1)}(\Gamma_l\ell_1)} = iZ_{l0}(\ell_1/\ell)\frac{H_1^{(1)}(\Gamma_l\ell_1)}{H_0^{(1)}(\Gamma_l\ell_1)} \tag{369}$$

Now for $\Gamma_l\ell_1 << 1$ (this complex value does not in general match the antenna, although perhaps by selection of appropriate values of Y_l and Γ_l we can get close with the real part?)

$$Z_i \sim \frac{1}{Y_l\ell}\frac{-i2/\pi}{1+i(2/\pi)\ln(\Gamma_l\ell_1 e^\gamma/2)} \tag{370}$$

with

$$Z_L = V(\ell)/I(\ell) = \frac{\Gamma_l}{Y(\ell)}\frac{H_1^{(1)}(\Gamma_l\ell)}{H_0^{(1)}(\Gamma_l\ell)} = \frac{\Gamma_l}{Y_l}\frac{H_1^{(1)}(\Gamma_l\ell)}{H_0^{(1)}(\Gamma_l\ell)} = iZ_{l0}\frac{H_1^{(1)}(\Gamma_l\ell)}{H_0^{(1)}(\Gamma_l\ell)} \tag{371}$$

or

$$Z_L \sim Z_{l0} \tag{372}$$

Note that

$$Z_L/Z_i \sim Z_{l0}Y_l\ell i\frac{\pi}{2}\left[1+i(2/\pi)\ln(\Gamma_l\ell_1 e^\gamma/2)\right]$$

$$\sim \frac{\pi}{2}\Gamma_l\ell\left[1+i(2/\pi)\ln(\Gamma_l\ell_1 e^\gamma/2)\right] >> 1 \tag{373}$$

and thus we have a growth of the impedance from the left end to the right end of the line.

References

[1] K. S. H. Lee (editor), **EMP Interaction: Principles, Techniques, and Reference Data**, Washington, DC: Hemisphere Pub. Corp., 1986, Section 1.3.2.

[2] K. S. H. Lee, "Two Parallel Terminated Conductors In External Fields," IEEE Transactions on Electromagnetic Compatibility, Vol. EMC-20, No. 2, May 1978, pp. 288-296.

[3] S. Ramo, J. R. Whinnery, and T. Van Duzer, **Fields And Waves In Communication Electronics**, New York: John Wiley & Sons, 1965.

[4] A. von Hippel (editor), **Dielectric Materials and Applications**, Boston: Artech House, 1954.

[5] M. E. Van Valkenburg, **Reference Data for Engineers: Radio, Electronics, Computer, & Communications**, Prentice Hall Pub., 1993.

[6] L. K. Warne and S. Campione, "Formulas For Plane Wave Coupling To A Transmission Line Above Ground With Terminating Loads," SAND2018-8736, August 2018.

[7] L. K. Warne, W. A. Johnson, L. I. Basilio, W. L. Langston, and M. B. Sinclair, "Subcell Method For Modeling Metallic Resonators In Metamaterials," PIER B, Vol. 38, pp. 135-164, 2012.

[8] L. K. Warne, "Asymptotic Expansion Of The Impedance Per Unit Length For Rectangular Conductors," Sandia National Laboratories Report, SAND2022-13840, October 2022.

[9] L. K. Warne, "Eddy Current Power Dissipation at Sharp Corners," IEEE Transactions On Microwave Theory And Techniques, Vol. 42, No. 2, Feb. 1994, pp. 283-290.

[10] L. K. Warne and W. A. Johnson, "Asymptotic Expansion Of The Impedance Per Unit Length of Thin Strip Conductors," Sandia National Laboratories Report, SAND2025-07333, June 2025.

[11] L. A. Vainshtein, "Calculation of ohmic losses at the edges of thin metal strips," Sov. Phys., Dokl. 31(8), August 1986.

[12] L. K. Warne and W. A. Johnson, "Eddy Current Power Dissipation At The Edge Of A Thin Conductive Layer," Sandia National Laboratories Report, SAND2022-13913, October 2022.

[13] W. R. Smythe, **Static and Dynamic Electricity**, New York: Hemisphere Pub. Corp., 1989, p. 102.

[14] M. Abramowitz and I. A. Stegun (editors), **Handbook of Mathematical Functions**, New York: Dover, 1972, Chapter 17.

[15] W. Hilberg, "From Approximations to Exact Relations for Characteristic Impedances," IEEE Transactions On Microwave Theory And Techniques, Vol. MTT-17, No. 5, May 1969.

[16] L. K. Warne, R. E. Jorgenson, J. T. Williams, L. I. Basilio, W. L. Langston, R. S. Coats, S. Campione, and K. C. Chen, "A Bound On Electromagnetic Penetration Through A Slot Aperture With Backing Cavity," SAND2016-9029, Sept. 2016.

[17] L. K. Warne, W. A. Johnson, B. F. Zinser, W. L. Langston, R. S. Coats, I. C. Reines, J. T. Williams, L. I. Basilio, and K. C. Chen, "Narrow Slot Algorithm," SAND2020-3979, April 2020.

[18] L. K. Warne, A. R. Pack, L. San Martin, and W. L. Langston, "Deep Slot Transmission And Receiving Cross Sections," SAND2025-02473, February 2025.

[19] L. K. Warne, R. E. Jorgenson, and H. G. Hudson, "Electromagnetic Field Limits Set By The V-Curve, SAND2014-5038, July 2014.

[20] K. S. H. Lee and F. C. Yang, "Trends and Bounds in RF Coupling to a Wire Inside a Slotted Cavity," IEEE Transactions On Electromagnetic Compatibility, Vol. 34, No. 3, Aug. 1992.

[21] L. K. Warne, K. S. H. Lee, H. G. Hudson, W. A. Johnson, and R. E. Jorgenson, and S. L. Stronach, "Statistical Properties of Linear Antenna Impedance in an Electrically Large Cavity," IEEE Trans. on Antennas and Propagation, Vol. 51, No. 5, May 2003.

[22] Department of Defense Interface Standard Electromagnetic Environmental Effects Requirements for Systems, MIL-STD-464C, 1 December 2010.

[23] S. Campione and L. K. Warne, "Penetration through slots in overmoded cavities," IEEE Transactions on Electromagnetic Compatibility, DOI:10.1109/TEMC.2021.3067005 (2021).

[24] L. K. Warne, W. L. Langston, L. I. Basilio, and W. A. Johnson, "First Principles Cable Braid Electromagnetic Penetration Model," PIER B, Vol. 66, pp. 63-89, 2016.

[25] L. K. Warne, W. L. Langston, L. I. Basilio, W. A. Johnson, and S. Campione, "First Principles Cable Braid Electromagnetic Penetration Model - Potential Impedance Clarification," SAND2025-09259, July 2025.

[26] L. K. Warne and A. R. Pack, "Low Frequency Cable Dual Shield Penetration Using Complete Transfer Immittance Model, SAND2025-07338, June 2025.

[27] T. Kley, "Optimized Single-Braided Cable Shields," IEEE Transactions On Electromagnetic Compatibility," Vol. 35, No. 1, February 1993, pp. 1-9.

DISTRIBUTION

Email—Internal

Name	Org.	Sandia Email Address
K. O. Merewether	02900	MS0405
W. L. Langston	01324	MS1152
E. A. Dohme	01324	MS1152
J. D. Kotulski	01324	MS1152
A. R. Pack	01322	MS1152
R. A. Pfeiffer	01324	MS1152
L. San Martin	01322	MS1152
L. K. Warne	01324	MS1152
Technical Library	01911	sanddocs@sandia.gov

Hardcopy—Internal

Number of Copies	Name	Org.	Mailstop
1	W. L. Langston	01324	MS1152
1	L. San Martin	01322	MS1152
6	L. K. Warne	01324	MS1152

Sandia National Laboratories

Sandia National Laboratories is a multimission laboratory managed and operated by National Technology & Engineering Solutions of Sandia LLC, a wholly owned subsidiary of Honeywell International Inc. for the U.S. Department of Energy's National Nuclear Security Administration under contract DE-NA0003525.